ENGINEERING TRANSACTIONS • *Engng. Trans.* • **49**, 2–3, 241–281, 2001
Polish Academy of Sciences • Institute of Fundamental Technological Research
10.24423/6x8q-2p37

MODELLING ELASTIC BEHAVIOUR OF SOFT TISSUES PART II. TRANSVERSE ISOTROPY

S. JEMIOŁO [1] and J. J. TELEGA [2]

[1] **INSTITUTE OF STRUCTURAL MECHANICS**
WARSAW UNIVERSITY OF TECHNOLOGY
al. Armii Ludowej 16, 00–637 Warsaw, Poland
e-mail: s.jemiolo@il.pw.edu.pl

[2] **INSTITUTE OF FUNDAMENTAL TECHNOLOGICAL RESEARCH**
POLISH ACADEMY OF SCIENCES
ul. Świętokrzyska 21, 00–049 Warsaw, Poland
e-mail: jtelega@ippt.gov.pl

New constitutive relationships for hyperelastic transversely isotropic materials have been proposed. The well-known isotropic hyperelastic model due to OGDEN [I.58] has been extended to transverse isotropy. It has been shown that some models intended to describe the nonlinear elastic behaviour of soft tissues are oversimplified and lead to incorrect results. An overview of soft tissue modelling, being a continuation of the one started in [48], has also been given.

1. INTRODUCTION

In the first part of the paper [48], new constitutive relationships applicable to isotropic, hyperelastic soft tissues have been proposed. Molecular and macroscopic models of skeletal muscle contraction have also been reviewed.

It is well-known that soft tissues usually exhibit anisotropic behaviour, see the next section for a brief review. For instance, the anisotropy may be due to the presence of oriented fibres like in skeletal muscles. Hence a natural need for studying transversely isotropic soft tissues. Other factors like the porosity, poroelasticity, and viscoelasticity also play a role in macroscopic behaviour of soft tissues, see the relevant references cited in Part I of our paper [48]. Similarly

to bone tissue, the mechanical behaviour of soft tissue is influenced by age and drugs. As in [48] we shall mainly focus on elastic behaviour of soft tissue though papers dealing with inelastic properties will also be mentioned.

Our aim is also to show that the anisotropic models proposed in [I.50, I.53, I.69] are insufficient to describe properly soft tissue behaviour, particularly in the range of small strains. Similar criticism applies to many oversimplified models where some invariants are absent and consequently, the number of material parameters is too small. Prior to the presentation of our original results, in Sec. 2, we shall complete the review started in the first part of the paper. Roman numerals refer to Part I of our paper.

2. Brief overview of soft tissue behaviour: continuation

This section is confined to phenomenological (macroscopic) behaviour of soft tissues. However, let us mention also the paper by Hajjar *et al.* [33] where a direct method of estimating the sarcomere length was proposed. In a series of papers [18 – 20], the formation of the power spectrum of extracellular potentials produced by a skeletal muscle fibre of finite length was analysed.

2.1. New experimental devices

Ortt *et al.* [70] described the design and construction of a new device capable of both in-plane biaxial testing and measurement of the spatial thermal diffusivity tensor, cf. Fig. 1. This device enables to investigate elastomers and planar soft tissues.

Dokos *et al.* [21] described a shear-test device for soft biological tissues capable of applying simple shear deformations simultaneously in two orthogonal directions, while measuring the resulting forces generated in three directions. The system was designed to apply shear in more than one principal direction so that the degree of anisotropy of the test specimen could be directly addressed.

Experimental data on certain soft tissues will be occasionally mentioned in the sequel. Here we only mention the investigation by Derwin and Soslowsky [17]. These authors investigated the hypothesis that mean collagen fibril diameter in the mouse tail tendon fascicle model is correlated with mechanical properties. The fascicle model was chosen in that it addresses the limitations of many previous structure-function models by providing a well-defined "representative volume" of tendon extracellular matrix such that direct quantitation and comparison of structure-function parameters is possible. The results obtained showed that fascicle stiffnes and maximum load are positively and moderately correlated with

mean fibril diameter. On the other hand, fascicle material properties, modulus and maximum stress, were only weakly correlated with mean fibril diameter.

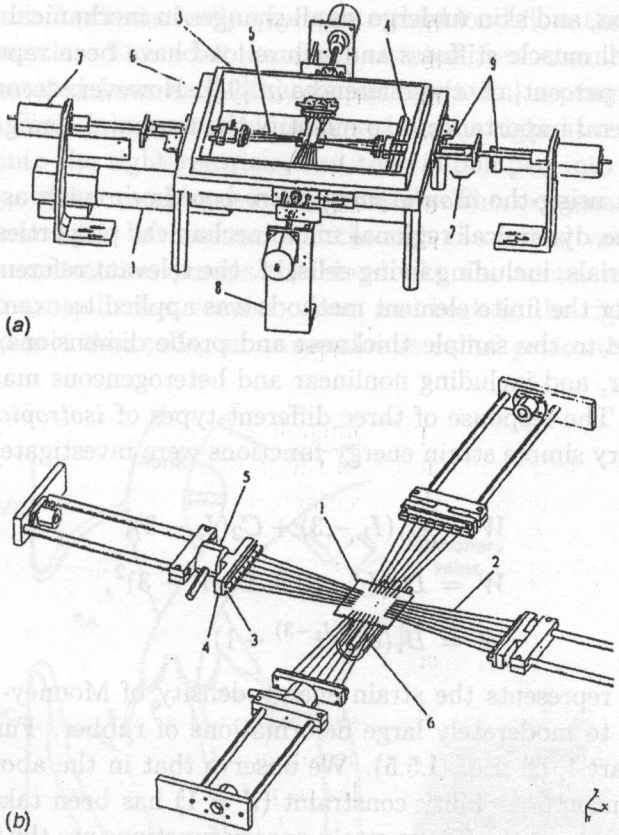

FIG. 1. Biaxial extension device. Panel (a) is an oblique view of the device where (1) camera, (2) load carriage, (3) environmental chamber, (4) heater, (5) Kevlar threads, (6) load frame, (7) motors, (8) motor supports, and (9) limit switches; in plane directions defined as 1 and 2. Panel (b) is a schema of (1) the specimen with centrally placed tracking markers, (2) Kevlar threads, (3) T-bar, (4) coupling bar, (5) load cell and (6) flash-bulb and reflector, as seen from below, after ORTT *et al.* [70].

MYERS *et al.* [64] determined the effect of average strain rate on the engineering stress-large strain properties of simulated and passive rabbit skeletal muscle (21 New Zealand white rabbits). Statistically significant effect of rate of loading (1/s, 10/s, 25/s) on the stress-strain responses of passive skeletal muscle was assessed. In the case of simulated muscle, the rate dependence was less pronounced.

VAN EE *et al.* [94] studied the time-dependent properties of skeletal muscle through the perimortem and postmortem periods using an animal model (12

New Zealand white rabbits). In addition, these authors examined the effects of preconditioning and freezing on the postmortem properties of skeletal muscle. In the previously published papers it is claimed that while the tissues of bone, ligament, tendon, and skin undergo small changes in mechanical properties postmortem, skeletal muscle stiffness and failure load have been reported to vary on the order of 50 percent, cf. the references in [94]. However, according to the last authors, of general importance is to quantify the temporal changes and the effect of freezing.

Indentation using the *atomic force microscope* is evolving as a powerful tool for studying the dynamical regional micromechanical properties of a variety of biological materials, including living cells, cf. the relevant references cited in [14]. In the last paper the finite element methods was applied to examine large indentations, relative to the sample thickness and probe dimensions, using an acute conical indenter, and including nonlinear and heterogeneous material properties of the sample. The response of three different types of *isotropic* materials characterized by very simple strain energy functions were investigated, see also [I.48]

$$W = C_1(I_1 - 3) + C_2(I_2 - 3), \tag{2.1}$$

$$W = D_1(I_1 - 3) + D_2(I_1 - 3)^2, \tag{2.2}$$

$$W = B_1(e^{B_2(I_1-3)} - 1). \tag{2.3}$$

Function (2.1) represents the strain energy density of Mooney-Rivlin model [I. 10], applicable to moderately large deformations of rubber. Function (2.3) was discussed in Part I, cf. Eq. (I.5.5). We observe that in the above strain energy functions the incompressibility constraint ($J = 1$) has been taken into account. It means that arguments of these strain energy functions are the invariants of isochoric deformation, see Eqs. $(I.4.7)_{1,2}$, and Eqs. $(5.10)_{1,4}$ in Sec. 5 of the present paper. It seems that only function (2.3) is applicable to modelling elastic behaviour of soft tissues. The two remaining strain energy functions do not predict significant stress increase in the range of relatively large deformations. We observe that polynomial strain energy functions for soft tissues should usually include the first invariant of isochoric deformation in the power higher than two.

2.2 Heart

An important problem in soft tissue mechanics is obtaining a mathematical description for the material properties of such tissues. Particularly, the material properties of the heart wall (myocardium) constitute a great problem in cardiac mechanics. The papers [32, 41, 59, 62, 65, 80, 86, 98] may be viewed as the-state-of-the-art in cardiac mechanics up to the year 1990. More precisely, SMAILL and

HUNTER [80] describe the structural arrangement of the cardiac muscle cells in the ventricular wall and the complex connective tissue matrix. For a brief description of geometry and materials of the heart, the reader is referred to FUNG [I.15, I.16]. Figure 2 schematically represents the blood flow through the heart and papillary muscle. The adult human heart has four chambers: two thin-walled atria separated from each other by an interatrial septum. As is shown schematically in Fig. 2, the venous blood flows into the right atrium, through the tricuspid value into the right ventricle, and then is pumped into the pulmonary artery and lung, where the blood is oxygenated. The oxygenated blood then flows from veins into the left atrium, and through the mitral valve into the left ventricle, whose contraction pumps the blood into the aorta, and then to the arteries, arterioles, capillaries, venules, veins, and back to the right atrium. The heart is wrapped in a thin collagenous membrane called *pericardium.*

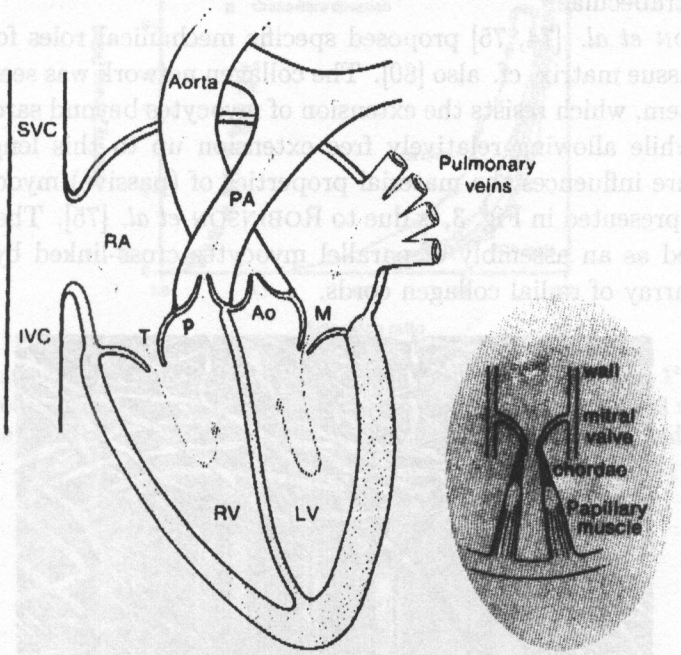

FIG. 2. Blood flow through the heart. The arrows shows the direction of blood flow; SVC-superior vena cava, IVC-inferior vena cava, RA- right atrium, RV- right ventricle, PA- pulmonary artery, LV- left ventricle, T- tricuspid, P- pulmonary, AO- aortic, M-mitral, after FUNG [I.16].

The cardiac muscle cell or *myocyte* is the main structural component of myocardium occupying around 70% of ventricular wall volume under normal circumstances. Cardiac myocytes resemble ellipsoid cylinders with a major-axis dimension of 1 to 10 μm and a length of 80 to 100 μm. Myocyte insert end

to end and each is connected with several others to form a three-dimensional network of cells. The interface between adjacent cells is referred to as the *intercalated disc* and the structure and properties of this region are of considerable importance.

ROBINSON *et al.* [74] classified the hierarchy of cardiac connective tissue organisation as "endomysium", "perimysium" and "epimysium", using terminology more commonly associated with skeletal muscle, cf. [48]. The cardiac endomysium incorporates the system of radial collagen cords together with a pericellular network of fibres that encompass the myocyte and a lattice of collagen fibrils and microthreads. In the context of heart, the term perimysium is used to describe the extensive meshwork of connective tissue that surrounds groups of cells and connections between contiguous cell bundles. The epimysium is defined as the sheath of connective tissue that surrounds entire muscles, for instance, papillary muscle and trabeculae.

ROBINSON *et al.* [74, 75] proposed specific mechanical roles for the cardiac connective tissue matrix, cf. also [80]. The collagen network was seen as a "strain-locking" system, which resists the extension of myocytes beyond sarcomere length of 2.2 μm while allowing relatively free extension up to this length. Cardiac microstructure influences the material properties of (passive) myocardium. One such model, presented in Fig. 3, is due to ROBINSON *et al.* [75]. The myocardium is represented as an assembly of parallel myocytes cross-linked by a uniformly distributed array of radial collagen cords.

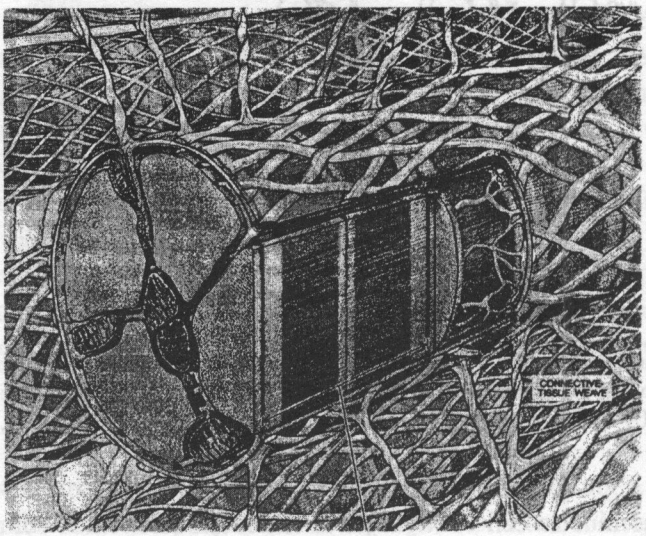

FIG. 3. Schematic representation of cardiac microstructure incorporating the collagen network surrounding myocytes and the radial collagen cords that interconnect myocytes, after ROBINSON *et al.* [75].

Various mechanical tests have been performed on specimens excised from various part of cardiac muscle. Here we deliver only two results depicted in Figs. 4 and 5. The experimental procedure leading to these results is described in [80]. The specimens were excised from six dog hearts. In Fig. 5 we present results for a specimen taken from the middle of the left ventricular wall subjected to 10 cycles of equibiaxial force loading with a cycle period of 30 sec. For other experimental data the reader is referred to the sequel of our paper and to [5, 48, 77]. The aim of papers [5, 77] was to specialize biaxial testing techniques for both the natural and glutaraldehyde-treated porcine aortic valve, and to apply these methods to generate sufficient planar mechanical property data for constitutive modelling.

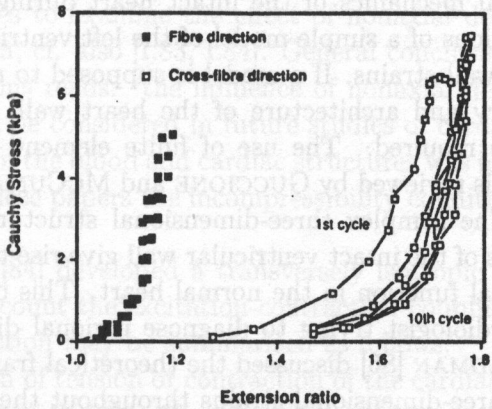

FIG. 4. Stress-extension relations for left ventricular midwall specimen during 1st, 9th and 10th cycles of equibiaxial loading. Cycle period 30 sec. and specimen thickness 1.83 mm. The solid lines indicate the order of loading in the cross-fibre directions, after SMAILL and HUNTER [80].

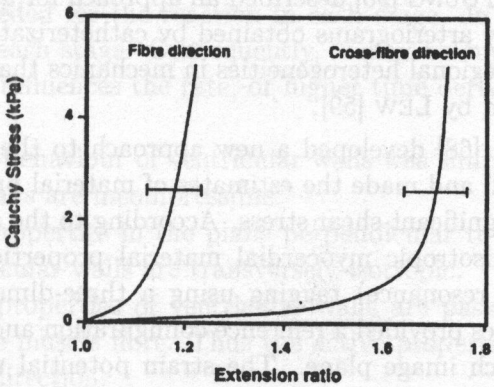

FIG. 5. Mean stress-extension relations for ventricular midwall specimens undergoing equibiaxial loading. Cycle period 10 sec., n-4, and mean specimen thickness 2.06 mm. The bars indicate ±1 standard deviation, after SMAILL and HUNTER [80].

HORWITZ [41] presented a microstructural model for the mechanical properties of the myocardium based on this type of information. It is assumed that the main structural elements of the myocardium are the interconnected networks of muscle fibers and collagen fibers, and the fluid matrix that embeds them. LANIR approach [I.44] was followed in order to derive a material law. HUMPHREY *et al.* (see their paper in [I.17]) outlined a formalism for identifying the constitutive law for the resting heart muscle based on an extensive program of mechanical testing, cf. also [I.28]. The mechanics of the myocardium as a muscle capable of active contraction and relaxation was outlined by NIELSEN and HUNTER [65]. These authors presented experimental and analytical methods for identifying the time-varying properties of active cardiac muscle. MCCULLOCH and OMENS [62] described the regional mechanics of the intact heart during passive filling and compared the predictions of a simple model of the left ventricle with experimental measurements of wall strains. If a model is supposed to represent accurately the complex geometry and architecture of the heart wall, however, computational techniques are required. The use of finite element methods in cardiac mechanics modelling is reviewed by GUCCIONE and MCCULLOCH in [32], cf. also MACKERLE [101]. The complex three-dimensional structure and time-varying mechanical properties of the intact ventricular wall give rise to significant heterogeneities of mechanical function in the normal heart. This can pose substantial difficulties to the cardiologist trying to diagnose regional disorders from radiographic images. WALDMAN [86] discussed the theoretical framework of kinematics as the basis for three-dimensional strains throughout the wall of the beating heart – both normal and diseased. These methods rely on the use of radiopaque implants in experimental animals, but natural landmarks on the heart offer the prospect of measuring regional mechanics in patients using conventional clinical imaging techniques. YOUNG [98] described an approach for analysing ventricular strains using coronary arteriograms obtained by catheterization. The functional consequences of the regional heterogeneities in mechanics that occur in the heart disease were discussed by LEW [59].

OKAMOTO *et al.* [68] developed a new approach to the mechanical testing of the ventricular wall and made the estimates of material properties for passive myocardium under significant shear stress. According to the authors, their study is the first where anisotropic myocardial material properties were determined from MR (magnetic resonance) tagging using a three-dimensional FE model. The MR tagged images provided a reference configuration and multiple deformed configurations for each image plane. The strain potential was assumed in the following form

$$W(\mathbf{E}) = C(e^{Q} - 1), \tag{2.4}$$

where

$$(2.5) \qquad Q = b_f E_{ff}^2 + b_t(E_{cc}^2 + E_{rr}^2 + E_{cr}^2 + E_{rc}^2) + b_{fs}(E_{fc}^2 + E_{cf}^2 + E_{fr}^2 + E_{rf}^2).$$

Here E_{ff} is fiber strain, E_{cc} is cross-fiber in-plane strain, E_{rr} is radial strain, E_{cr} is shear strain in the cross-fiber-radial coordinate plane, and E_{fc} and E_{fr} are shear strains in the fiber-cross-fiber and fiber-radial coordinate planes, respectively. Thus the anisotropic model considered involves four material constants: C, b_f, b_t, and b_{fs}.

ZAHALAK and DE LABORDERIE [99] incorporated a three-dimensional generalization of the HUXLEY [I.31] cross-bridge theory in a finite element model of ventricular mechanics to examine the effect of nonaxial deformations on active stress in myocardium, cf. also [I.83, I.84]. General conclusion resulting from the performed calculations reads: "the influence of nonaxial deformations on active muscle stress should be considered in future studies of cardiac mechanics".

The interaction of the blood and cardiac structures was investigated in [44, 57, 58]. In the first of these papers the incompressibility condition, usually assumed, is questioned.

TANAKA *et al.* [84] developed a transversely isotropic model of ventricular walls, taking into account the excitation-contraction coupling. The phenomenon of excitation-contraction may be summarized as follows:

a) The generation of tension or contraction of the cardiac muscle is controlled by the concentration of Ca^{++} in the cell.

b) There are threshold and saturated values in the response for the concentration of Ca^{++}.

c) In the process mentioned, the subsequent stage is caused by the preceding one, and time is needed for the reaction in each stage. In other words, a time delay is induced in each stage. Consequently, it may be supposed that the concentration of Ca^{++} influences the rate, or higher time derivatives of the tension or contraction.

The mechanical behaviour of ventricular walls was simplified as follows:

i) Ventricular walls are incompressible.

ii) Mechanical properties in the plane perpendicular to the muscle fiber are isotropic, i.e., ventricular walls are transversely isotropic.

iii) Mechanical properties of ventricular walls are passive in the directions perpendicular to the muscle fibre. Thus the active properties are observed only in the muscle fibre direction.

iv) Viscoelastic properties of ventricular walls can be neglected.

v) The stress acting on the ventricular walls is expressed as the sum of passive stress $\mathbf{T}^p$ and active stress $\mathbf{T}^a$; that is the second Piola-Kirchhoff stress tensor $\mathbf{T}$

is given by

$$\mathbf{T} = \mathbf{T}^a + \mathbf{T}^p. \tag{2.6}$$

The passive stress $\mathbf{T}^p$ may be expressed by

$$\mathbf{T}^p = \frac{\partial(\rho_0 W)}{\partial \mathbf{E}}. \tag{2.7}$$

The strain energy density function $\rho_0 W$ is a particular case of formula (7.3) below and is assumed in the form

$$\rho_0 W(\mathbf{E}) = a \exp\psi(\mathbf{E}) + p[\det(2\mathbf{E} + \mathbf{I}) - 1], \tag{2.8}$$

where ρ_0 denotes the mass density in the undeformed configuration, a is a material constant, and p denotes the Lagrange multiplier (the pressure). Following CHUONG and FUNG [11], in [84] it is assumed that ψ is the quadratic form of the Green strain tensor $\mathbf{E}$.

According to the previous assumption (iii), the active stress $\mathbf{T}^a$ can be expressed by

$$\mathbf{T}^a = \tau^a \mathbf{M}, \tag{2.9}$$

where $\mathbf{M} = \mathbf{m} \otimes \mathbf{m}$ is the structural tensor (see Sec. 4), and τ^a is the activated stress caused by the activation. The maximum value of τ^a depends on the length of the cardiac muscle because the maximum number of cross-bridges between myosin and actin filaments, which determines the maximum value of the tension, changes with the length of the muscle, cf. Part I of our paper. The magnitude of tension is also governed by the activity that expresses the ratio of bonding of troponin with Ca^{++}, that is, the ratio of active filaments. The activity and the strain of muscle fibres are denoted by α and E_h, respectively. It can be shown that

$$E_h = \mathbf{E}\mathbf{m} \cdot \mathbf{m}. \tag{2.10}$$

Suppose that the cardiac muscle is soaked in Ca^{++} solution of a constant concentration for a sufficiently long time under the condition of constant length. Consequently, the active stress τ^a will tend to the asymptotic value τ^{as}. It may be assumed that

$$\tau^{as} = \hat{\tau}^{as}(E_h, \alpha) = \tau^{as}_{\max} F(E_h) A(\alpha). \tag{2.11}$$

The current value of active stress is a solution of the following simple evolution equation

$$\dot{\tau}^a = \frac{d\tau^a}{dt} = b(\tau^{as} - \tau^a), \tag{2.12}$$

where b is a material constant specifying the rate of change. We observe that the last equation has to be completed by the initial condition, say $\tau^a(0) = \tau_0$. Equation (2.12) is a particular case of more general relation

$$\dot{\tau}^a = f(t, \tau^{as} - \tau^a). \tag{2.13}$$

The functions F, A are assumed to be specified by

$$F(E_h) = \left\langle (1 + F_0)\exp\left\{ -\left[\frac{E_h - E_{h0}}{\Delta E_h}\right]^2 \right\} - F_0 \right\rangle, \tag{2.14}$$

$$A(\alpha) = \langle 1 - \exp[-m(\alpha - \alpha_{ths})] \rangle, \tag{2.15}$$

respectively. Here E_{h0} is the value of E_h at the maximum tension, ΔE_h is one half of the range of E_h generating the tension, and F_0 is the material coefficient. The symbol $\langle \cdot \rangle$ denotes the Macauley bracket. Equation (2.15) was formulated with reference to the relationships between the tension and the concentration of Ca^{++} at the saturated state. Moreover, m is the material constant and α_{ths} is the value corresponding to the threshold of Ca^{++} that can generate the tension.

The evolution equation

$$\dot{\alpha} = c(\beta - a), \tag{2.16}$$

yields satisfactory predictions for the experimental data. Here β denotes the concentration of Ca^{++}, and c is the material coefficient. The last equation is viewed as describing the diffusion of Ca^{++} and the bonding of troponin. Exploiting the experimental data, due to CANNEL *et al.* [7], for cardiac muscle of mice, the concentration β was assumed in the following form:

$$\beta = \beta_0 t^k \exp(-lt), \tag{2.17}$$

where β_0, k, and l are material constants.

The calculations were performed by assuming that $\psi(\mathbf{E})$ is given by the Saint-Venant Kirchhoff isotropic model (this fact was not explicitly stated), cf. [I.10, 4],

$$\psi(\mathbf{E}) = \lambda(\mathrm{tr}\mathbf{E})^2 + 2\mu \mathrm{tr}\mathbf{E}^2. \tag{2.18}$$

Further, it was assumed that $\lambda = 34.0$, $\mu = 5.0$, $a = 0.2$ [kPa], $\tau^{as}_{\max} = 107.9$ [kPa], $E_{h0} = 0.322$, $\Delta E_h = 0.205$, $F_0 = 0.032$, $m = 0.16 \left[\frac{1}{\mathrm{mM}}\right]$, $\alpha_{ths} = 0.56$ [mM], $\beta_0 = 0.0326 \left[\frac{\mathrm{mM}}{(\mathrm{ms})^k}\right]$, $k = 1.0$, $l = 0.004 \left[\frac{1}{\mathrm{ms}}\right]$, $b = 0.007 \left[\frac{1}{\mathrm{ms}}\right]$, $c = 0.018 \left[\frac{1}{\mathrm{ms}}\right]$. Typical results for $A(\alpha) = 1$ are presented in Fig. 6.

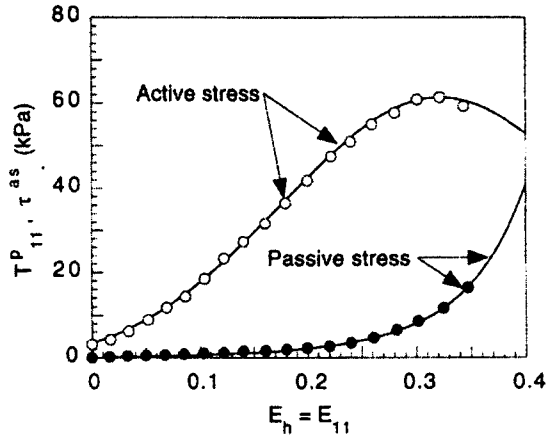

FIG. 6. Passive stress versus cardiac muscle fibre strain relationship (*solid line* calculated result; *solid circles* experimental data) and relationship of maximum of the isometric tension versus cardiac muscle fibre strain (*solid line* calculated result; *open circles* experimental data of the papillary muscles of a cat, after TANAKA *et al.* [84].

2.3. Arterial walls

One of frequently studied soft tissue are arteries (arterial walls) since their biomechanical properties are crucial for understanding the changes in the cardiovascular system due to age, arteriosclerosis and hypertension; cf. [15, 35 – 40] and the references therein. Figure 7 presents an idealized model of the arterial wall. The intima I is the innermost layer consisting of a single layer of endothelial cells that rests on a thin basal membrane and a subendothelial layer whose thickness varies with topography, age and disease. The media M is composed of smooth muscle cells, a network of elastin and collagen fibrils and elastic laminae which separate M into a number of fiber-reinforced layers. The primary constituents of the adventitia A are thick bundles of collagen fibrils; A is the outermost layer surrounded by loose connective tissue. Thus a vascualar tissue is a highly complex material containing collagen, elastin and smooth muscle, cf. [I.27] and the references therein. For the literature related to experimantal studies of blood vessels the reader is referred to many references cited by VOSSOUGHI and TÖZEREN [I.75]. Also, these authors performed ingenious shear tests which provide useful information on material parameters and described the experimental procedure. Of interest is the fact that *rectangular* aortic and rubber specimens were investigated. Figure 8 shows typical shear stress versus shear strain curves for three aortic rectangular specimens from aorta No 1. Each data point corresponds to externally applied stress level. It was found that the relationships between shear stress and shear strain for all the aortic specimens tested were *linear*, cf. Figs. 8, 9. This is despite the fact that the relationships between the normal stress and

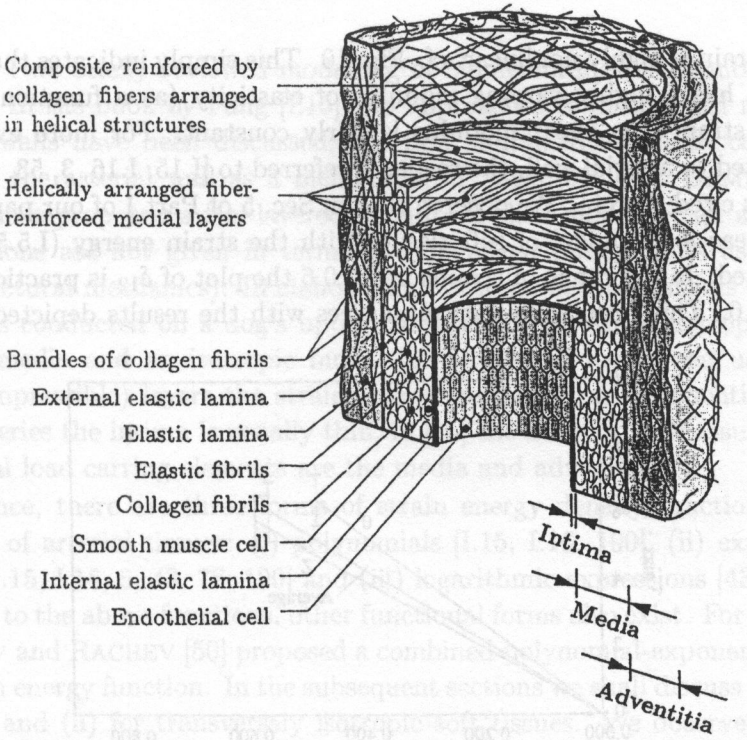

FIG. 7. Diagrammatic model of the major components of a healthy artery composed of three layers: intima (I), media (M) and adventitia (A), after HOLZAPFEL *et al.* [38].

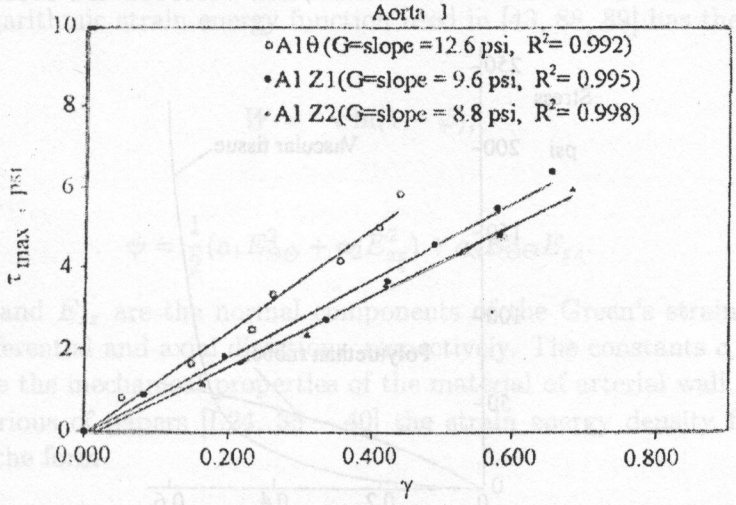

FIG. 8. Typical shear stress versus shear strain diagrams for aorta No 1 for both θ and z-specimens. Slopes of the least squared lines provided the effective shear modulus for the material of the aorta, after VOSSOUGHI and TÖZEREN [I.75].

normal strain is highly nonlinear, cf. Fig. 10. This simply indicates that although the aorta has a highly varying modulus of elasticity (as a function of applied stress or strain), its shear modulus is fairly constant. For more experimental data related to arterial wall, the reader is referred to [I.15, I.16, 3, 53, 56] and the references cited therein. We observe that in Sec. 5 of Part I of our paper [48] the simple shear for a model of soft tissues with the strain energy (I.5.5) has been investigated. In the range of strains up to 0.6 the plot of δ_{12} is practically linear, cf. Fig. I.6. This result qualitatively agrees with the results depicted in Figs. 9 and 10.

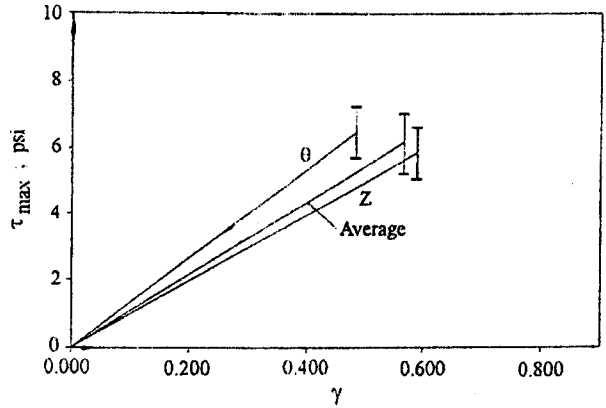

FIG. 9. An average shear stress versus shear strain curve for bovine aorta. The average covers 5 specimens in θ-direction and 13 in z-direction, after VOSSOUGHI and TÖZEREN [I.75].

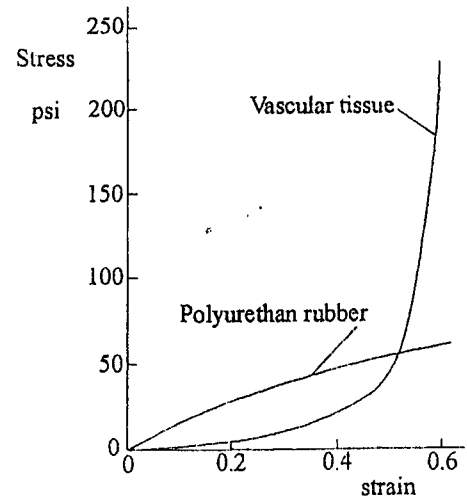

FIG. 10. A typical normal stress versus normal strain curve for bovine aortic tissue exhibiting highly nonlinear behaviour. In addition, such stress-strain curve for polyurethane rubber is also shown, after VOSSOUGHI and TÖZEREN [I.57].

In Part I we briefly reviewed modelling of biomembranes as membranes, cf. [I.26, I.29]. In the book by Fung [I.15] two approaches to mechanical modelling of arterial walls have been discussed; the first simplified approach consists in considering the arterial wall as a membrane, cf. also [36, 66]. DEMIRAY and VITO [15] have proposed a two-layered cylindrical shell model for an aorta (the shell equations are not given in terms of generalized forces, as is usually the case in structural mechanics). In elaboration of the model the authors exploited their results conducted on a dog's upper thoracic aorta. An orthotropic elastic model for media and an isotropic model for adventitia have been used. For both (incompressible) layers the strain energy functions are exponential. Since in large arteries the intima is usually thin, in [15] the authors have assumed that the essential load carring elements are the media and adventitia.

In essence, there are three forms of strain energy density function for the description of arterial tissues: (i) polynomials [I.15, I.16, 100], (ii) exponential functions [I.15, I.16, 5, 43, 78, 100] and (iii) logarithmic expressions [43, 88, 89]. In addition to the above functions, other functional forms also exist. For instance, KAS'YANOV and RACHEV [50] proposed a combined polynomial-exponential form of the strain energy function. In the subsequent sections we shall discuss functions of type (i) and (ii) for transversely isotropic soft tissues. We observe that the above classification of hyperelastic strain energy functions applies likewise to other soft tissues, for instance to the myocardium characterized by the stored energy functions of type (i), and more frequently, of type (ii).

The logarithmic strain energy function used in [43, 88, 89] has the following form

$$W = -c\ln(1-\psi), \tag{2.19}$$

where

$$\psi = \frac{1}{2}(a_1 E_{\Theta\Theta}^2 + a_2 E_{zz}^2) + a_3 E_{\Theta\Theta} E_{zz}. \tag{2.20}$$

Here $E_{\Theta\Theta}$ and E_{zz} are the normal components of the Green's strain tensor in the circumferential and axial directions, respectively. The constants c, a_1, a_2, a_3 characterize the mechanical properties of the material of arterial wall.

In a serious of papers [I.24, 35 – 40] the strain energy density function is written in the form

$$W = W_{iso} + W_{aniso}. \tag{2.21}$$

Here the first term represents the isotropic contribution whilst the second one describes the anisotropic contribution. The function W_{aniso} is assumed in the form similar to the classical approach of fibre-reinforced materials, since anisotropic

soft tissues possess fibres. In the papers mentioned, currently used forms of W were discussed, and results of many numerical calculations were provided.

As we already know, soft tissues often reveal a hysteretic behaviour, modelled by a pseudo-elastic response, cf. [I.15, I.16, 84]. However, no general approach to pseudo-elastic modelling of such tissues seems to be available. It seems, that the paper by OGDEN and ROXBURGH [67], developed for isotropic rubber-like materials offers new insight into modelling of pseudo-elastic response of soft tissues. In [67] the energy function $W(\mathbf{F}, \eta)$ depends on an additional variable η, interpreted as a damage parameter. It seems reasonable to assume that

$$\dot{\eta} = \frac{d\eta}{dt} = f(t, \eta, \mathbf{F}), \tag{2.22}$$

plus an initial condition. Treated as a damage parameter, η assumes values between 0 and 1.

An important, and still weakly recognized, is the interaction blood-arterial wall (fluid-solid interaction). Usually, one assumes that the blood is a Navier-Stokes fluid while arterial walls are supposed either to be isotropic and hyperelastic [2, 85] or anisotropic [100]. Blood-arterial wall interactions are important in investigation and modelling of atherosclerosis (stenotic tubes), cf. also [3, 8].

Finally, we should mention inelastic behaviour of arterial walls, both viscoelastic [37, 100] and viscoplastic [84].

3. RESIDUAL STRESSES IN STRAINS IN SOFT TISSUES

As a rule, both the bone tissue and soft tissues are inhomogeneous and anisotropic and change during their lifetime. Hence it is not surprising that in such tissues residual stresses have been discovered. According to FUNG [I.16], residual stresses were discovered independently by VAISHNAV and VOSSOUGHI [92], who found them in blood vessels, and his former student P. Patitucci jointly with him, who discovered such stresses in the left ventricle of a rabbit in 1982.

In this section we shall review the papers on residual stresses and strains in soft tissues. Their role in tissues is not quite clear. In 1983 FUNG [I.16] formulated the "principle of optimal operation" stating that each organ operates in such a manner as to achieve optimal performance. Unfortunately, no mathematical model of this principle is available, at least as far as we know. On the other hand, TAKAMIZAWA and HAYASHI [89, 90] and TAKAMIZAWA and MATSUDA [91] proposed the "uniform strain" theory.

OMENS and FUNG [69] quantitatively described the two-dimensional residual strains in the equatorial slice of the rat left ventricle. In this paper five adult male (200 – 300g) Sprague Dawley rats were anesthetized. Their left ventricles were

cut into 2 – 3 mm thick equatorial slices. Next, radial cuttings were performed, cf. Fig. 11. A simple quantitative measure that reflects the residual strain distribution in a slice of the left ventricle is the opening angle, see Fig. 12C. The mean initial opening angle from 11 of these slices was $45 \pm 10°$. However, the opening angle was inreasing during the entire data acquisition period, presumably due to ischemic contracture. OMENS *et al.* [102] continued this study by measuring left ventricular geometry and opening angles in rats spanning a large range of ventricular size and shape, and relatively small alterations in passive myocardial material properties (79 Sprague Dawley rats of either sex ranging from 32 to 492 grams). These authors showed that physiologic left ventricular remodelling in rats decreases myocardial residual strain in proportion to the relative reduction in wall thickness-radius ratio. SUMMER *et al.* [81] found that opening angles were significantly higher in ischemic hearts than in sham-operated or strain-softened hearts, suggesting that acute coronary artery occlusion may significantly increase residual stress and strain in the left ventricles of rats. A total of 47 rats were used and divided into three groups: ischemic, sham-operated, and strain-softened.

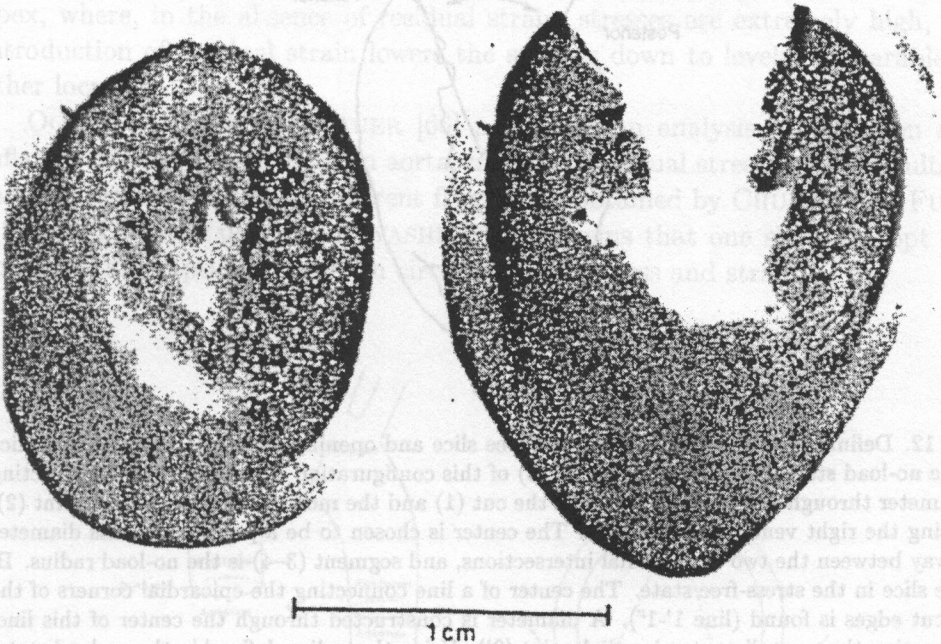

FIG. 11. Equatorial slices of a rat heart showing imbedded microspheres. The photograph on the left is before radial cutting (no-load state) and that on the right is after radial cutting (stress-free state), after OMENS and FUNG [69].

TAKAMIZAWA and MATSUDA [91] developed a general theory employing the uniform strain hypothesis and applied it to the left ventricle.

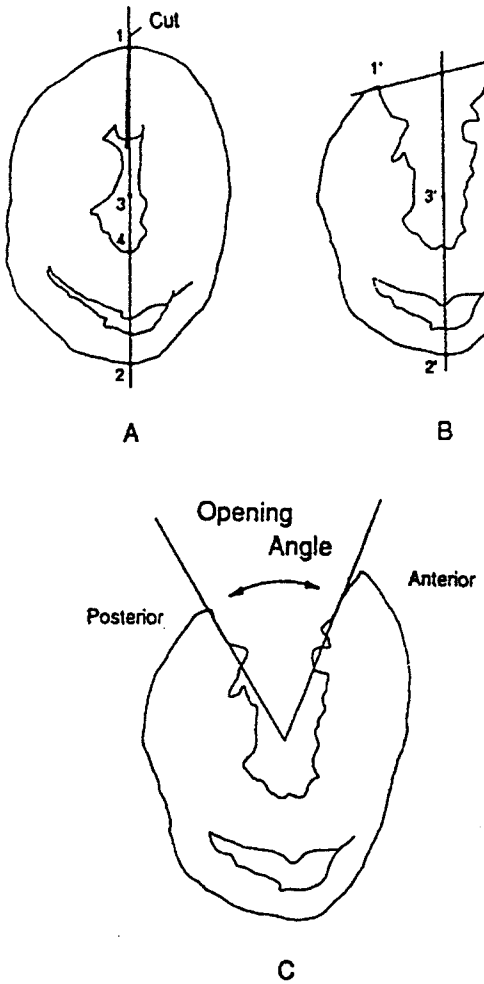

FIG. 12. Definition of the center of a stress-free slice and opening angle. A: Drawing of a slice in the no-load state. The chamber center (3) of this configuration is estimated by constructing a diameter through the epicardial edge of the cut (1) and the most distant epicardial point (2), crossing the right ventricular chamber. The center is chosen to be a point along this diameter midway between the two endocardial intersections, and segment (3–4) is the no-load radius. B: Same slice in the stress-free state. The center of a line connecting the epicardial corners of the two cut edges is found (line 1'-1"). A diameter is constructed through the center of this line, intersecting the most distant epicardial point (2'). Using the radius defined in the no-load state, the center of the stress-free configuration (3') is chosen to at be the same distance from the septal endocardium along its diameter. Papillary muscles were ignored in these measurements. C: Opening angle, defined as the angle between the two radial lines connecting the center of the ventricular chamber and the centerlines of the walls at the cut edges. Note the asymmetry of the posterior and anterior free walls, after OMENS and FUNG [69].

Let us pass to residual stresses and strains in arteries. In the seminal paper by VAISHNAV and VOSSOUGHI [92] nine aortas (3 bovine and 6 porcine) were investigated. The maximum magnitudes of the circumferential engineering strains through the wall thickness varied from 0.044 to 0.124, and the corresponding stresses varied from 44 to 12 G/cm^2, where an approximate value of the Young modulus of 10^3 G/cm^2 was used. For further developments and results the reader is referred to [12, 13, 26, 30, 34, 60, 61, 71, 93, 96]. Particularly, LIU and FUNG [60] performed experimental investigations of Sprague Dawley rat heart and aorta, see Fig. 13. The thickness of specimens was 1 mm. Figure 14 represents photographs of some typical cut specimens.

TAKAMIZAWA and HAYASHI [90] showed, on the uniform strain hypothesis, that when an arterial wall is unloaded and cut longitudinally, its cross-section becomes a sector and the strain and stress remaining before cutting are completely relieved, cf. also [89].

DELFINO *et al.* [I.12] performed observations on 10 pig carotid bifurcations arteries. The results showed that the effect of residual strain is to make the stress distribution uniform throughout the carotid bifurcation artery. Especially at the apex, where, in the absence of residual strain, stresses are extremely high, the introduction of residual strain lowers the stresses down to levels comparable to other locations.

OGDEN and SCHULZE-BAUER [66] performed an analysis of extension and inflation of a tube, modelling an aorta, including residual stresses. The results of calculations yielded results different from those obtained by CHUONG and FUNG [13] and TAKAMIZAWA and HAYASHI [89]. It seems that one should adopt the combined assumption of uniform circumferential stress and strain.

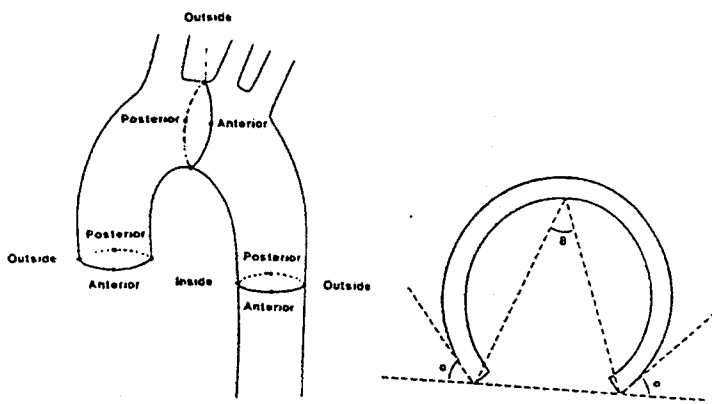

FIG. 13. Left: Nomenclature for sites: "anterior", "posterior", "inside", and "outside". Right: Definition of the opening section angle θ and the sum of the angles between the tangents to the vessel section at the site of the cut and the x-axis, α; after LIU and FUNG [60].

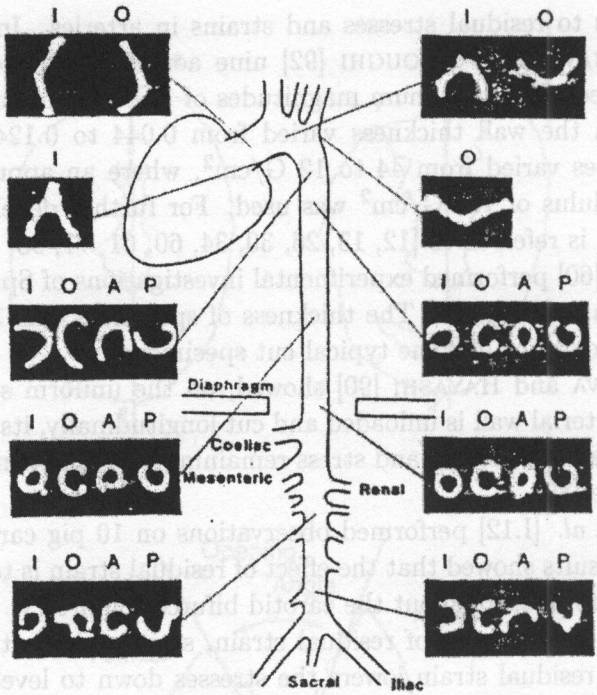

FIG. 14. Photographs of the zero-stress configurations of short segments of aorta along the aortic tree. The symbols A, P, I, O stand for anterior, posterior, inside and outside, respectively, see Fig. 13; after LIU and FUNG [60].

GREGERSEN *et al.* [31] investigated esophagi of guinea pigs. The experimental procedure used was similar to that used previously for arteries; we recall that the esophagus is a tube. The opening angle was found to be a function of time and location. At the no-load state, a tight buckling pattern was seen at the inner wall, indicating that the inner wall of the esophagus is compressed. Upon reducing the no-load state to the zero-stress state by cutting the ring, the opened ring expanded itself into a sector with an opening angle of about 80°. The buckling in the inner layer was still observed, though to a lesser degree. The buckling in the zero-stress state indicated that compression in the inner wall and tension in the outer wall were not completely relieved.

Upon removal of articular cartilage from the underlying subchondral bone, a "curling" of the cartilage sample is observed, cf. SETTON *et al.* [79] and the references therein. This behaviour was also observed in strips of human costal and nasal septum cartilage, cf. the references in [79]. This warping is attributed to residual stresses. SETTON *et al.* [79] defined parameters associated with cartilage curling and swelling ex situ that may be used to determine the magnitude and distribution of the swelling-induced residual strains in articular cartilage. Moreover,

the contributions of anisotropy and inhomegeneity for the surface zone cartilage to these swelling-induced residual strains were determined.

4. General relations

Let $\mathbf{F}$ denote the deformation gradient, $J = \det\mathbf{F}$ and $\mathbf{E} = (\mathbf{C} - \mathbf{I})/2$, where $\mathbf{C} = \mathbf{F}^T\mathbf{F}$ is the right Cauchy-Green tensor, cf. [I.10, I.58]. By $\mathbf{S}$, $\mathbf{T}$ we denote the first (unsymmetric) and second (symmetric) Piola-Kirchhoff stress tensor, respectively. We have

$$\mathbf{S} = \mathbf{FT}. \tag{4.1}$$

The Cauchy stress tensor $\boldsymbol{\sigma}$ in the deformed configuration is defined by

$$\boldsymbol{\sigma} = \frac{1}{J}\mathbf{S}\mathbf{F}^T. \tag{4.2}$$

To describe the transverse isotropy we introduce a parametric tensor $\mathbf{M} = \mathbf{m} \otimes \mathbf{m}$. The tensor $\mathbf{M}$ is prescribed in the initial (Lagrangian) configuration. The unit vector $\mathbf{m}(\mathbf{X})$ coincides with the direction of material fibres in the initial configuration; $\mathbf{X}$ denotes the Lagrangian variable of a material point. Let

$$S = \{\mathbf{Q} \in O(3) | \mathbf{M} = \mathbf{Q}\mathbf{M}\mathbf{Q}^T\}, \tag{4.3}$$

where $O(3)$ stands for the full orthogonal group in the three-dimensional case, cf. [I.37]. The stored energy density function W satisfies

$$W(\mathbf{E}, \mathbf{M}, r) = W(\mathbf{Q}\mathbf{E}\mathbf{Q}^T, \mathbf{M}, r) = \tilde{W}(\mathbf{C}, \mathbf{M}, r) = \tilde{W}(\mathbf{Q}\mathbf{C}\mathbf{Q}^T, \mathbf{M}, r), \quad \forall \mathbf{Q} \in S. \tag{4.4}$$

Here the function $r(\mathbf{X})$ describes the inhomogeneity of the material. From the point of view of tensor functions and constitutive equations, the variable r is not essential. Therefore we shall only consider homogeneous materials.

The theory of representation of transversely isotropic functions yields, cf. [I.37],

$$W(\mathbf{E}, \mathbf{M}) = \breve{W}(N_i) = \tilde{W}(\mathbf{C}, \mathbf{M}) = \hat{W}(I_i); \qquad i = 1, ..., 5. \tag{4.5}$$

Here $\{N_i\}$ and $\{I_i\}$ denote the so-called basic invariants of the tensors $\mathbf{E}$ and $\mathbf{C}$, respectively. The constitutive equations are

$$\mathbf{T} = \breve{\mathbf{T}}(\mathbf{E}) = \frac{1}{2}\left(\frac{\partial \breve{W}}{\partial \mathbf{E}} + \frac{\partial \breve{W}}{\partial \mathbf{E}^T}\right) = \frac{1}{2}\sum_{i=1}^{5} \frac{\partial \breve{W}}{\partial N_i}\left(\frac{\partial N_i}{\partial \mathbf{E}} + \frac{\partial N_i}{\partial \mathbf{E}^T}\right) = \sum_{i=1}^{5} \alpha_i \mathbf{G}_i^{(\mathbf{E})}, \tag{4.6}$$

$$\mathbf{T} = \check{\mathbf{T}}(\mathbf{C}) = \frac{\partial \hat{W}}{\partial \mathbf{C}} + \frac{\partial \hat{W}}{\partial \mathbf{C}^T} = \sum_{i=1}^{5} \frac{\partial \hat{W}}{\partial I_i}\left(\frac{\partial I_i}{\partial \mathbf{C}} + \frac{\partial I_i}{\partial \mathbf{C}^T}\right) = \sum_{i=1}^{5} 2\beta_i \mathbf{G}_i^{(\mathbf{C})}. \tag{4.7}$$

The symmetric tensors of the second-order $\mathbf{G}_i^{(\mathbf{E})}$ and $\mathbf{G}_i^{(\mathbf{C})}$ are the so-called generators, cf. [I.37].

We assume the existence of a natural state where

$$W(\mathbf{0}, \mathbf{M}) = \tilde{W}(\mathbf{I}, \mathbf{M}) = 0, \qquad \check{\mathbf{T}}(\mathbf{0}) = \hat{\mathbf{T}}(\mathbf{I}) = \mathbf{0}. \tag{4.8}$$

The basic invariants of the function $\check{W}(N_i)$ are well-known [I.37]. We write

$$\check{W}(N_i) = \check{W}(\mathrm{tr}\mathbf{E}, \mathrm{tr}\mathbf{E}^2, \mathrm{tr}\mathbf{E}^3, \mathrm{tr}\mathbf{E}\mathbf{M}, \mathrm{tr}\mathbf{E}^2\mathbf{M}), \qquad i = 1, ..., 5. \tag{4.9}$$

The quadratic approximation of the last function leads to the Saint-Venant Kirchhoff stored energy function, in general anisotropic (transversely isotropic). We denote this stored energy function by W_{SVK}. We have

$$\check{W}(N_i) = W_{SVK}(N_i(\mathbf{E})) + O(\|\mathbf{E}\|^3), \qquad i = 1, 2, 4, 5. \tag{4.10}$$

Similarly to the isotropic Saint-Venant Kirchhoff model [I.10], the function W_{SVK} is assumed to be convex with respect to $\mathbf{E}$, i.e., the following fourth-order tensor

$$\frac{1}{4}\left(\frac{\partial^2 W_{SVK}(N_i(\mathbf{E}))}{\partial \mathbf{E} \otimes \partial \mathbf{E}} + \frac{\partial^2 W_{SVK}(N_i(\mathbf{E}))}{\partial \mathbf{E}^T \otimes \partial \mathbf{E}} + \frac{\partial^2 W_{SVK}(N_i(\mathbf{E}))}{\partial \mathbf{E} \otimes \partial \mathbf{E}^T} + \frac{\partial^2 W_{SVK}(N_i(\mathbf{E}))}{\partial \mathbf{E}^T \otimes \partial \mathbf{E}^T}\right), \qquad i = 1, 2, 4, 5, \tag{4.11}$$

has to be positive definite. The stored energy function W_{SVK} is given by

$$\tilde{W}_{SVK}(\mathbf{E}) = W_{SVK}(N_i(\mathbf{E})) = a_1(\mathrm{tr}\mathbf{E})^2 + a_2\mathrm{tr}\mathbf{E}^2 + a_3(\mathrm{tr}\mathbf{E}\mathbf{M})^2 + a_4\mathrm{tr}\mathbf{E}\mathrm{tr}\mathbf{E}\mathbf{M} + a_5\mathrm{tr}\mathbf{E}^2\mathbf{M}. \tag{4.12}$$

For an isotropic material, the strain energy density (2.18) can be obtained from relationship (4.12) provided that $a_1 = \lambda$, $a_2 = 2\mu$, $a_3 = a_4 = a_5 = 0$.

Substituting (4.12) into (4.6) we find the constitutive relationship for transversely isotropic Saint-Venant Kirchhoff material in the Lagrangian description. The reader is advised to find the classical relationship $\mathbf{T} = \mathbf{S} \cdot \mathbf{E} = (S_{ijkl}E_{kl})$ in arbitrary coordinates. We observe that for incompressible, transversely isotropic Saint-Venant Kirchhoff materials only four material coefficients amongst $a_1, ..., a_5$ are independent.

5. New constitutive relationships for transversely isotropic hyperelastic materials

In this section we are going to present new models of transversely isotropic hyperelastic materials.

The stored energy function $\hat{W}$ for compressible materials can equivalently be written as follows:

$$\hat{W}(I_i) = \hat{W}(\mathrm{tr}\mathbf{C}, \mathrm{tr}\,\mathrm{Cof}\,\mathbf{C}, \det\mathbf{C}, \mathrm{tr}(\mathbf{MC}), \mathrm{tr}(\mathbf{MCofC})), \tag{5.1}$$

where

$$\mathrm{Cof}\mathbf{C} = (\det\mathbf{C})\mathbf{C}^{-1}. \tag{5.2}$$

Hence

$$\mathbf{T} = 2\beta_1\mathbf{I} + 2\beta_2(I_2\mathbf{I} - \mathrm{Cof}\mathbf{C})\mathbf{C}^{-1} + 2(\beta_3 I_3 + \beta_5 I_5)\mathbf{C}^{-1} + 2\beta_4\mathbf{M} - \beta_5 I_3(\mathbf{MC}^{-1} + \mathbf{C}^{-1}\mathbf{M}). \tag{5.3}$$

The scalar functions β_i depend on I_i, $i = 1, ..., 5$.

In the Eulerian description we have

$$\boldsymbol{\sigma} = 2\left(\frac{I_2}{J}\beta_2 + J\beta_3 + \frac{I_5}{J}\beta_5\right)\mathbf{I} + \frac{2\beta_1}{J}\mathbf{B} - 2\beta_2 J\mathbf{B}^{-1} + 2\beta_4\tilde{\mathbf{M}} - J\beta_5(\tilde{\mathbf{M}}\mathbf{B}^{-1} + \mathbf{B}^{-1}\tilde{\mathbf{M}}), \tag{5.4}$$

where

$$\mathbf{B} = \mathbf{F}\mathbf{F}^T, \qquad \tilde{\mathbf{M}} = \mathbf{F}\mathbf{M}\mathbf{F}^T. \tag{5.5}$$

According to $(5.5)_2$ the material fibres are rotated and stretched. We now propose two new stored energy functions for transversely isotropic materials:

$$\hat{W}(I_i) = \sum_{i+j+l+k\neq 0} A_{ijkl}(I_1 - 3)^{a_i}(I_2 - 3)^{b_j}(I_4 - 1)^{c_j}(I_5 - 1)^{d_j} + \Gamma(I_3), \tag{5.6}$$

$$\hat{W}(I_i) = \sum_{i+j+l+k\neq 0} B_{ijkl}(I_1^{a_i} - 3^{a_i})(I_2^{b_j} - 3^{b_j})(I_4^{c_j} - 1)(I_5^{d_j} - 1) + \Gamma(I_3), \tag{5.7}$$

Here the coefficients A_{ijkl} and B_{ijkl} are not the components of tensors but merely material parameters. The coefficients a_i, b_j, c_k and d_l are additional parameters which have to be determined by using experimental data and nonlinear optimization. The function $\Gamma(I_3)$ with $\Gamma(1) = 0$ is convex and tends to infinity for I_3 tending to zero and infinity.

Having in mind applications and finite element algorithms [1, 46, 47, 97], it is convenient to choose transversely isotropic invariants of $\mathbf{C}$ for incompressible materials in a manner enabling to formulate the constitutive relationships in a uniform manner. Recalling that $\mathbf{F} = \mathbf{RU} = \mathbf{VR}$ [I.10, I.58] and performing the multiplicative decomposition of $\mathbf{F}$ on volumetric and distorsional parts, we write

$$\mathbf{F} = J^{1/3}\overline{\mathbf{F}} = J^{1/3}\mathbf{R}\overline{\mathbf{U}} = J^{1/3}\overline{\mathbf{V}}\mathbf{R}, \quad \det\overline{\mathbf{F}} = \det\overline{\mathbf{U}} = \det\overline{\mathbf{V}} = 1. \tag{5.8}$$

The stored energy function is postulated as follows:

$$\overline{W}(\overline{I}_j, J) = \overline{W}(\mathrm{tr}\overline{\mathbf{C}}, \mathrm{tr}\ \mathrm{Cof}\overline{\mathbf{C}}, \mathrm{tr}(\mathbf{M}\overline{\mathbf{C}}), \mathrm{tr}(\mathbf{M}\mathrm{Cof}\overline{\mathbf{C}}), J), \quad j = 1, ..., 4, \tag{5.9}$$

where

$$\begin{aligned}
\overline{I}_1 &= \mathrm{tr}\overline{\mathbf{B}} = \mathrm{tr}\overline{\mathbf{C}} = J^{-\frac{2}{3}} I_1, \quad I_1 = \mathrm{tr}\mathbf{C} = \mathrm{tr}\mathbf{B}, \quad \mathbf{B} = \mathbf{F}\mathbf{F}^T, \\
\overline{I}_2 &= \mathrm{tr}\overline{\mathbf{B}}^{-1} = \mathrm{tr}\overline{\mathbf{C}}^{-1} = J^{-\frac{4}{3}} I_2, \quad I_2 = \mathrm{tr}\ \mathrm{Cof}\mathbf{C} = \frac{1}{2}(I_1^2 - \mathrm{tr}\mathbf{C}^2), \\
&\qquad \mathrm{tr}\mathbf{C}^2 = \mathrm{tr}\mathbf{B}^2, \\
\overline{I}_3 &= \mathrm{tr}(\mathbf{M}\overline{\mathbf{C}}) = J^{-\frac{2}{3}}\mathrm{tr}(\mathbf{M}\mathbf{C}) = J^{-\frac{2}{3}}\mathrm{tr}\tilde{\mathbf{M}}, \\
\overline{I}_4 &= \mathrm{tr}(\mathbf{M}\mathrm{Cof}\overline{\mathbf{C}}) = J^{-\frac{4}{3}}\mathrm{tr}(\mathbf{M}\mathrm{Cof}\mathbf{C}) = J^{-\frac{4}{3}}\mathrm{tr}(\mathrm{Cof}\tilde{\mathbf{M}}), \qquad \tilde{\mathbf{M}} = \mathbf{F}\mathbf{M}\mathbf{F}^T.
\end{aligned} \tag{5.10}$$

The invariants I_1, I_2 and J^2 are the so-called basic invariants used for isotropic materials, cf. [I.10, I.58].

After standard calculations one can derive the corresponding constitutive relationships in the Lagrangian and Eulerian descriptions. Details are left to the reader.

We now propose two stored energy functions for incompressible and nearly incompressible transversely isotropic, hyperelastic materials, cf. Eqs. (5.5), (5.6),

$$\overline{W}(\overline{I}_j, J) = \sum_{i+j+l+k\neq 0} \overline{A}_{ijkl}(\overline{I}_1 - 3)^{\alpha_i}(\overline{I}_2 - 3)^{\beta_j}(\overline{I}_3 - 1)^{\gamma_j}(\overline{I}_4 - 1)^{\delta_j} + \overline{\Gamma}(J), \tag{5.11}$$

$$\overline{W}(\overline{I}_j, J) = \sum_{i+j+l+k\neq 0} \overline{B}_{ijkl}(\overline{I}_1^{\alpha_i} - 3^{\alpha_i})(\overline{I}_2^{\beta_j} - 3^{\beta_j})(\overline{I}_3^{\gamma_j} - 1)(\overline{I}_4^{\delta_j} - 1) + \overline{\Gamma}(J). \tag{5.12}$$

For incompressible materials $\overline{\Gamma}(J) = \lambda(J - 1)$, where λ denotes the Lagrange multiplier associated with the condition $J = 1$.

For incompressible and nearly incompressible transversely isotropic materials like soft tissues one can use the following stored energy function, cf. formula (7.3) below,

$$\overline{W}_{NTF}(\overline{I}_i) = \sum_{j=1}^{N} \overline{a}_j \left(e^{\overline{\psi}_j(\overline{I}_i)} - 1 \right) + \overline{\Gamma}(J), \qquad \overline{a}_j > 0. \tag{5.13}$$

In the case of incompressible materials and vanishing invariants $\overline{I}_3$ and $\overline{I}_4$, the relation (5.13) reduces to the known models of incompressible soft tissues, cf. Part I [48]. In a separate paper we shall discuss the form of the function $\overline{\Gamma}(J)$ used previously by various authors in the case of nearly incompressible materials. One might mention here the penalty method.

6. Generalization of isotropic Ogden's model to transversely isotropic hyperelastic materials

Our approach permits to extend the well-known Ogden's model [I.10, I.58] to transversely isotropic materials. We propose the following stored energy function:

$$\begin{aligned} W_{OG}(\mathbf{C},\mathbf{M}) = {} & \sum_{k=1}^{K} \hat{a}_k(\mathrm{tr}\mathbf{C}^{\alpha_k} - 3) + \sum_{l=1}^{L} \hat{b}_l(\mathrm{tr}\ \mathrm{Cof}\mathbf{C}^{\beta_l} - 3) \\ & + \sum_{m=1}^{M} \hat{c}_m[(\det\mathbf{C})^{\chi_m} - 1] + \sum_{n=1}^{N} \hat{d}_n(\mathrm{tr}\mathbf{M}\mathbf{C}^{\delta_m} - 1) \\ & + \sum_{p=1}^{P} \hat{e}_p(\mathrm{tr}\mathbf{M}\mathrm{Cof}\mathbf{C}^{\varepsilon_p} - 1) + \sum_{q=1}^{Q} \hat{f}_q[(\mathrm{tr}\mathbf{M}\mathbf{C}^{\phi_q})(\mathrm{tr}\mathbf{M}\mathbf{C}^{\varphi_q}) - 1] \\ & + \sum_{s=1}^{S} \hat{g}_s[(\mathrm{tr}\mathbf{M}\mathrm{Cof}\mathbf{C}^{\gamma_s})(\mathrm{tr}\mathbf{M}\mathrm{Cof}\mathbf{C}^{\eta_s}) - 1]. \end{aligned} \tag{6.1}$$

Ogden's stored energy function for the isotropic hyperelastic materials is recovered provided that $\hat{d}_n = 0$, $\hat{e}_p = 0$, $\hat{f}_q = 0$, $\hat{g}_s = 0$, $n = 1,...,N$; $p = 1,...,P$; $q = 1,...,Q$; $s = 1,...,S$, see [I.10, I.58]. We observe that the stored energy function (6.1) is not, in general, polyconvex in Ball's sense (for the notion of polyconvexity the reader is referred to the book by Ciarlet [I.10]). The problem of polyconvexity of the function (6.1) will be studied elsewhere. Here we only mention that for the anisotropic stored energy function involving fabric tensor, more appropriate seems to be the notion of anisotropic polyconvex func-

tions. For instance, in the case of transverse isotropy the stored energy function $\mathcal{W}(\mathbf{F}) = W(\mathbf{C}, \mathbf{M})$ is polyconvex provided that there exists a convex function

$$g : M^3 \times M^3 \times M^3 \times M^3 \times [0, +\infty) \to R$$

such that

$$\mathcal{W}(\mathbf{F}) = g(\mathbf{F}, \mathbf{MF}, \mathrm{Cof}\mathbf{F}, \mathrm{Cof}(\mathbf{MF}), \det\mathbf{F}),$$

for all $\mathbf{F} \in M^3_+$. Here M^3 denotes the space of real 3×3 matrices and $M^3_+ = \{\mathbf{F} \in M^3 | \det\mathbf{F} > 0\}$.

One can easily demonstrate, similarly to the case of isotropy, that the strain energy (4.12) describing transversely isotropic materials, is not polyconvex. Moreover, this function is also not rank-one convex. We observe that the convexity of the function (4.12) with respect to $\mathbf{E}$ renders the passage to the classical Hooke's law. The elastic moduli a_i, $i = 1, ..., 5$, are the same as in the linear theory.

For incompressible isotropic Ogden's materials we have $\mathrm{trCof}\overline{\mathbf{C}}^{\beta_l} = \mathrm{tr}\overline{\mathbf{C}}^{-\beta_l}$. Consequently, for such materials the stored energy function is simplified.

In the Lagrangian description the constitutive relationship is given by

$$\begin{aligned}
(6.2)\qquad \mathbf{T} = {} & 2\kappa\mathbf{C}^{-1} + \sum_{n=1}^{N} \hat{d}_n\delta_m(\mathbf{MC}^{\delta_m-1} + \mathbf{C}^{\delta_m-1}\mathbf{M}) \\
& + \sum_{p=1}^{P} \hat{e}_p\varepsilon_p \left[\left(\mathbf{M}(\mathrm{Cof}\mathbf{C}^{\varepsilon_p-1})\right)\mathbf{C}^{-1} + \mathbf{C}^{-1}((\mathrm{Cof}\mathbf{C}^{\varepsilon_p-1})\mathbf{M})\right] \\
& + \sum_{q=1}^{Q} \hat{f}_q \left[\phi_q \mathrm{trMC}^{\varphi_q}(\mathbf{MC}^{\phi_q-1} + \mathbf{C}^{\phi_q-1}\mathbf{M})\right. \\
& \left. + \varphi_q \mathrm{trMC}^{\phi_q}(\mathbf{MC}^{\varphi_q-1} + \mathbf{C}^{\varphi_q-1}\mathbf{M})\right] \\
& + \sum_{s=1}^{S} \hat{g}_s\gamma_s \mathrm{trMCof}\mathbf{C}^{\eta_s}\left[(\mathbf{M}(\mathrm{Cof}\mathbf{C}^{\gamma_s}))\mathbf{C}^{-1} + \mathbf{C}^{-1}((\mathrm{Cof}\mathbf{C}^{\gamma_s})\mathbf{M})\right] \\
& + \sum_{s=1}^{S} \hat{g}_s\eta_s \mathrm{trMCof}\mathbf{C}^{\gamma_s}\left[(\mathbf{M}(\mathrm{Cof}\mathbf{C}^{\gamma_s}))\mathbf{C}^{-1} + \mathbf{C}^{-1}((\mathrm{Cof}\mathbf{C}^{\gamma_s})\mathbf{M})\right],
\end{aligned}$$

where

$$\begin{aligned}
(6.3)\qquad \kappa = {} & \sum_{k=1}^{K} \hat{a}_k\alpha_k\mathbf{C}^{\alpha_k} + \sum_{l=1}^{L} \hat{b}_l\beta_l[(\mathrm{tr}\ \mathrm{Cof}\mathbf{C}^{\beta_l})\mathbf{I} - \mathrm{Cof}\mathbf{C}^{\beta_l}] + \sum_{m=1}^{M} \hat{c}_m\chi_m(\det\mathbf{C})^{\chi_m} \\
& + \sum_{p=1}^{P} \hat{e}_p\varepsilon_p(\mathrm{trMCof}\mathbf{C}^{\varepsilon_p}) + \sum_{s=1}^{S} \hat{g}_s(\gamma_s + \eta_s)(\mathrm{trMCof}\mathbf{C}^{\gamma_s})(\mathrm{trMCof}\mathbf{C}^{\eta_s}).
\end{aligned}$$

It is not difficult to pass to the constitutive relationship in the Eulerian description. This problem is left to the reader.

The condition (4.8) yields two additional relations between the material coefficients:

$$\sum_{k=1}^{K} \hat{a}_k \alpha_k + 2\sum_{l=1}^{L} \hat{b}_l \beta_l + \sum_{m=1}^{M} \hat{c}_m \chi_m + \sum_{p=1}^{P} \hat{e}_p \varepsilon_p + \sum_{s=1}^{S} \hat{g}_s(\gamma_s + \eta_s) = 0,$$

$$\sum_{n=1}^{N} \hat{d}_n \delta_m - \sum_{p=1}^{P} \hat{e}_p \varepsilon_p + \sum_{q=1}^{Q} \hat{f}_q(\phi_q + \varphi_q) + \sum_{s=1}^{S} \hat{g}_s(\gamma_s + \eta_s = 0. \tag{6.4}$$

The hyperelastic stored energy functions have to be such that their quadratic approximation with respect to $\mathbf{E}$ yields the Saint-Venant Kirchhoff model, in general anisotropic. Since the following formulae are valid:

$$\begin{aligned}
\mathrm{tr}\mathbf{C}^{\alpha} &= 3 + 2\alpha \mathrm{tr}\mathbf{E} + 2\alpha(\alpha - 1)\mathrm{tr}\mathbf{E}^2 + \dots, \\
\mathrm{tr}(\mathrm{Cof}\mathbf{C}^{\beta} &= 3 + 4\beta \mathrm{tr}\mathbf{E} + 2\beta^2(\mathrm{tr}\mathbf{E})^2 + 2\beta(\beta - 1)\mathrm{tr}\mathbf{E}^2 + \dots, \\
(\det\mathbf{C})^{\chi} &= 1 + 2\chi\left[\mathrm{tr}\mathbf{E} + \frac{1}{2}(\mathrm{tr}\mathbf{E})^2 - \mathrm{tr}\mathbf{E}^2\right] + \chi(2\chi - 1)(\mathrm{tr}\mathbf{E})^2 + \dots, \\
\mathrm{tr}\mathbf{M}\mathbf{C}^{\delta} &= 1 + 2\delta \mathrm{tr}\mathbf{M}\mathbf{E} + 2\delta(\delta - 1)\mathrm{tr}\mathbf{M}\mathbf{E}^2 + \dots, \\
\mathrm{tr}\mathbf{M}(\mathrm{Cof}\mathbf{C}^{\varepsilon}) &= 1 + 2\varepsilon(\mathrm{tr}\mathbf{E} - \mathrm{tr}\mathbf{E}^2) + 2\varepsilon^2(\mathrm{tr}\mathbf{E})^2 \\
&\quad - 2\varepsilon(1 + 2\varepsilon \mathrm{tr}\mathbf{E})\mathrm{tr}\mathbf{M}\mathbf{E} + 2\varepsilon(\varepsilon + 1)\mathrm{tr}\mathbf{M}\mathbf{E}^2 + \dots, \\
(\mathrm{tr}\mathbf{M}\mathbf{C}^{\phi})(\mathrm{tr}\mathbf{M}\mathbf{C}^{\varphi}) &= 1 + 2(\phi + \varphi)\mathrm{tr}\mathbf{M}\mathbf{E} + 4\phi\varphi(\mathrm{tr}\mathbf{M}\mathbf{E})^2 \\
&\quad + 2[\phi(\phi - 1) + \varphi(\varphi - 1)]\mathrm{tr}\mathbf{M}\mathbf{E}^2 + \dots, \\
(\mathrm{tr}\mathbf{M}\mathrm{Cof}\mathbf{C}^{\gamma})(\mathrm{tr}\mathbf{M}\mathrm{Cof}\mathbf{C}^{\eta}) &= 1 + 2(\gamma + \eta)(\mathrm{tr}\mathbf{E} - \mathrm{tr}\mathbf{E}^2) + 2(\gamma^2 + \eta^2)(\mathrm{tr}\mathbf{E})^2 \\
&\quad -2[\gamma(1 + 2\gamma \mathrm{tr}\mathbf{E}) + \eta(1 + 2\eta \mathrm{tr}\mathbf{E})]\mathrm{tr}\mathbf{M}\mathbf{E} + 2[\gamma(\gamma + 1) + \eta(\eta + 1)]\mathrm{tr}\mathbf{M}\mathbf{E}^2 \\
&\quad -8\gamma\eta \mathrm{tr}\mathbf{E}\mathrm{tr}\mathbf{M}\mathbf{E} + 4\gamma\eta[(\mathrm{tr}\mathbf{E})^2 - (\mathrm{tr}\mathbf{M}\mathbf{E})^2] + \dots,
\end{aligned} \tag{6.5}$$

therefore in Eq. (6.2) one can assume only one term in each sum to obtain the Saint-Venant Kirchhoff model. Taking into account (6.5) in (6.2) we obtain five additional relations between the material coefficients:

$$a_1 = 2\left[\sum_{l=1}^{L}\hat{b}_l\beta_l^2 + \sum_{m=1}^{M}\hat{c}_m\chi_m^2 + \sum_{p=1}^{P}\hat{e}_p\varepsilon_p^2 + \sum_{s=1}^{S}\hat{g}_s(\gamma_s+\eta_s)^2\right],$$

$$a_2 = 2\left[\sum_{k=1}^{K}\hat{a}_k\alpha_k(\alpha_k-1) + \sum_{l=1}^{L}\hat{b}_l\beta_l(\beta_l-2) - \sum_{m=1}^{M}\hat{c}_m\chi_m - \sum_{p=1}^{P}\hat{e}_p\varepsilon_p + \sum_{s=1}^{S}\hat{g}_s(\gamma_s+\eta_s)\right],$$

$$a_3 = 4\left(\sum_{q=1}^{Q}\hat{f}_q\phi_q\varphi_q - \sum_{s=1}^{S}\hat{g}_s\gamma_s\eta_s\right), \tag{6.6}$$

$$a_4 = -4\left[\sum_{p=1}^{P}\hat{e}_q\varepsilon_p^2 + \sum_{s=1}^{S}\hat{g}_s(\gamma_s+\eta_s)^2\right],$$

$$a_5 = 2\left\{\sum_{n=1}^{N}\hat{d}_n\delta_m(\delta_m-1) + \sum_{p=1}^{P}\hat{e}_p\varepsilon_p(\varepsilon_p-1) + \sum_{q=1}^{Q}\hat{f}_q[\phi_q(\phi_q-1)+\varphi_q(\varphi_q-1)] + \sum_{s=1}^{S}\hat{g}_s[\gamma_s(\gamma_s+1)+\eta_s(\eta_s+1)]\right\}.$$

Let us provide an example of the stored energy function applicable to modelling the incompressible and nearly incompressible transversely isotropic materials:

$$\overline{W}_{OG}(\overline{\mathbf{C}}, J, \mathbf{M}) = \sum_{k=1}^{K}\overline{a}_k(\mathrm{tr}\overline{\mathbf{C}}^{\alpha_k} - 3) + \sum_{l=1}^{L}\overline{b}_l(\mathrm{tr}\ \mathrm{Cof}\overline{\mathbf{C}}^{\beta_l} - 3) + \sum_{n=1}^{N}\overline{d}_n(\mathrm{tr}\mathbf{M}\overline{\mathbf{C}}^{\delta_m} - 1) + \sum_{p=1}^{P}\overline{e}_p(\mathrm{tr}\mathbf{M}\mathrm{Cof}\overline{\mathbf{C}}^{\varepsilon_p} - 1) + \sum_{q=1}^{Q}\overline{f}_q\left[(\mathrm{tr}\mathbf{M}\overline{\mathbf{C}}^{\phi_q})(\mathrm{tr}\mathbf{M}\overline{\mathbf{C}}^{\varphi_q}) - 1\right] + \sum_{s=1}^{S}\overline{g}_s\left[(\mathrm{tr}\mathbf{M}\mathrm{Cof}\overline{\mathbf{C}}^{\gamma_s})(\mathrm{tr}\mathbf{M}\mathrm{Cof}\overline{\mathbf{C}}^{\eta_s} - 1\right] + \overline{\Gamma}(J). \tag{6.7}$$

7. Comments on models proposed in [I.50, I.53, I.69]

Tong and Fung [I.69] proposed the following stored energy function for soft tissues:

$$W(\mathbf{E}) = \alpha(\mathbf{E}) + a_0\beta(\mathbf{E})e^{\psi(\mathbf{E})}, \tag{7.1}$$

where

$$\alpha(\mathbf{E}) = \frac{1}{2}\mathbf{E}\cdot\mathcal{U}\cdot\mathbf{E}, \quad \beta(\mathbf{E}) = \frac{1}{2}\mathbf{E}\cdot\mathcal{B}\cdot\mathbf{E}, \tag{7.2}$$

$$\psi(\mathbf{E}) = \operatorname{tr}(\mathbf{AE}) + \frac{1}{2}\mathbf{E}\cdot\mathcal{C}\cdot\mathbf{E} + \ldots.$$

Here $\mathcal{U}, \mathcal{B}$ and $\mathcal{C}$ are fourth-order tensors which are determined by materials parameters obtained from appropriate experiments. The function (7.1) is not, in general, polyconvex, and it has too many material parameters with similar mechanical interpretation. Also, it can be shown that this model exhibits drawbacks similar to the hyperelastic model of Saint-Venant Kirchhoff, cf. [I.10]. To yield reasonable results, the function $\psi(\mathbf{E})$ should involve tensors of order higher than four. The paper by Tong and Fung [I.69] has nevertheless played a role in revealing the possibility of modelling the nonlinear behaviour of soft tissues by means of exponential functions.

Our previous considerations suggest that a reasonable stored energy function for transversely isotropic hyperelastic soft tissues can be assumed in the following form

$$W(I_i) = \sum_{j=1}^{N} a_j(e^{\psi_j(I_i)} - 1), \qquad a_j > 0. \tag{7.3}$$

We observe that if the functions ψ_j are postulated as being independent of material parameters, then a_j can be determined by using linear optimization methods. Also, the function (7.3) is polyconvex provided that each function ψ_j is polyconvex.

Let us pass to the models proposed in [I.50, I.53]. In [I.50] the stored energy function is given by

$$W = C_1(e^{\psi} - 1), \tag{7.4}$$

where

$$\psi = C_2(I_1 - 3)^2 + C_3(I_1 - 3)(I_4 - 1) + C_4(I_4 - 1)^2. \tag{7.5}$$

Here C_i, $i = 1,...,4$, are material coefficients and $C_1 > 0$. The constitutive equation in Eulerian description expresses as follows:

$$\boldsymbol{\sigma} = -p\mathbf{I} + 2\beta_1\mathbf{B} + 2\beta_4\tilde{\mathbf{M}}, \tag{7.6}$$

where p denotes the Lagrange multiplier (pressure) and

$$\beta_1 = \frac{\partial W}{\partial I_1} = C_1 e^{\psi}[2C_2(I_1 - 3) + C_3(I_4 - 1)],$$

$$\beta_4 = \frac{\partial W}{\partial I_4} = C_1 e^{\psi}[C_3(I_1 - 3) + 2C_4(I_4 - 1)].$$

Obviously the material is incompressible. The quadratic approximation of (7.4) yields

$$W = C_1C_2(\mathrm{tr}\mathbf{E})^2 + C_1C_3\mathrm{tr}\mathbf{E}\mathrm{tr}\mathbf{E}\mathbf{M} + C_1C_4(\mathrm{tr}\mathbf{E}\mathbf{M})^2 + O(\|\mathbf{E}\|^3). \tag{7.7}$$

Function (7.7) does not contain a sufficient number of material parameters to predict mechanical properties of incompressible, transversely isotropic material in the range of relatively small deformations, in the case of 3D problems. From the representation theory of so-called plane (two-dimensional) tensor function follows that function (7.7) is an irreducible quadratic function of 2D tensor $\mathbf{E}$, cf. [I.37]. On the basis of the material parameters given in [I.50] for rabbit myocardium we have found, among others, the level sets depicted in Figs. 15, 16,

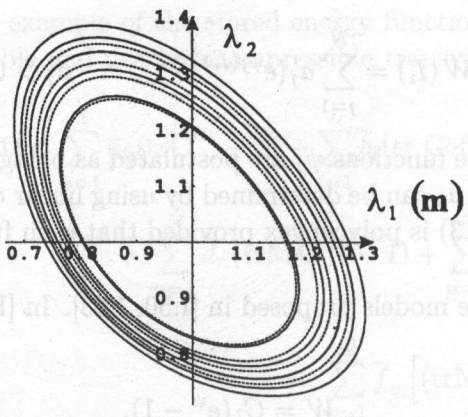

FIG. 15. Comparison of level sets for the stored energy function (7.4), (7.5) (dotted curves) with its quadratic approximation (7.7) (continuous curves) in the case of averaged values for 7 samples studied in [I.50]. The curves correspond to two-dimensional tests in the principal axes of anisotropy.

and the stored energy function for one-dimensional deformations presented in Fig. 17. To construct these figures we exploited the data given in [I.50] and gathered in Table 1. The scatter of the reported values is significant. Figure 17 shows that for relatively small values of stretches, the stored energy function, constructed in [I.50], may even assume negative values. We conclude that the constitutive modelling proposed in [I.50] is not sufficiently accurate.

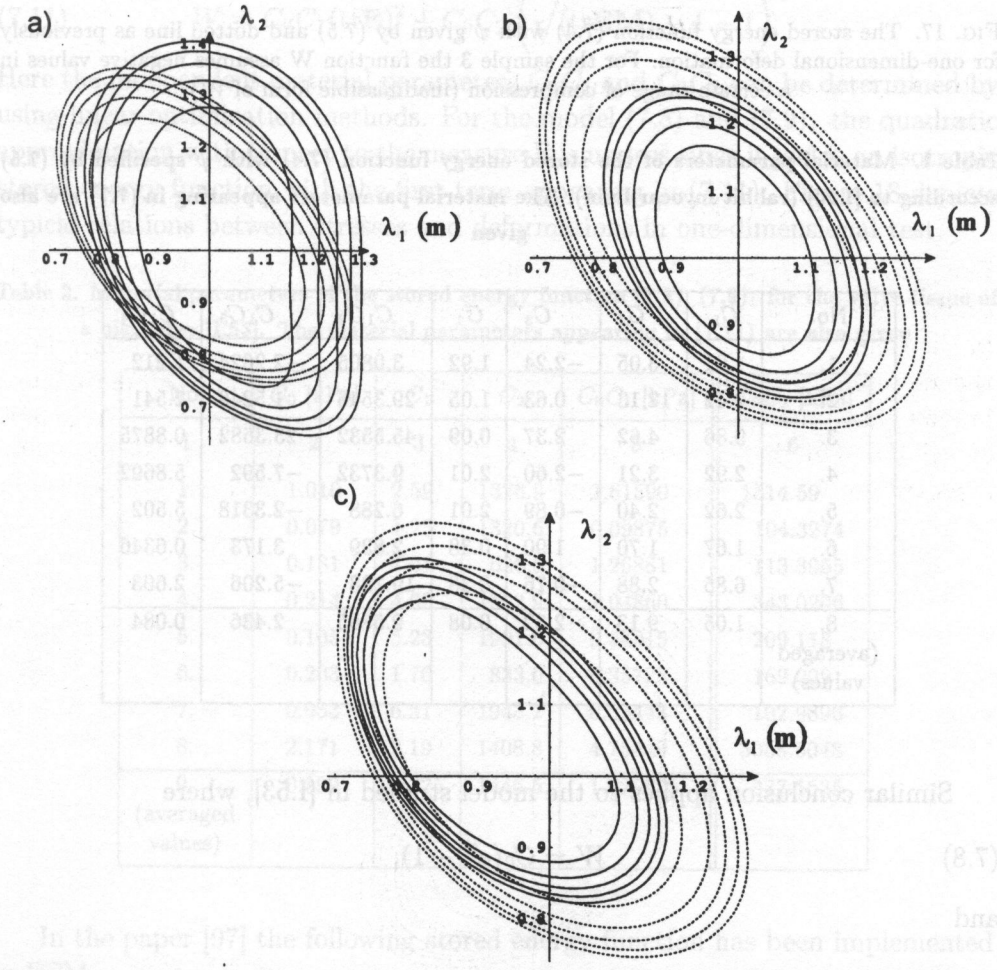

FIG. 16. Level sets for three samples and the stored energy function (7.4), (7.5); λ_1, λ_2 are principal stretches (two-dimensional tests) and the samples orientation coincides with the unit vector **m** describing the orientation of fibres: a) sample 1, b) sample 2, c) sample 3. The dotted lines correspond to "averaged" material parameters.

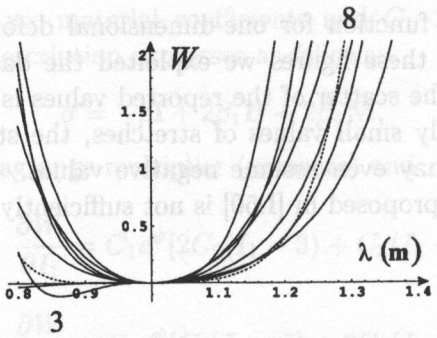

FIG. 17. The stored energy function (7.4) with ψ given by (7.5) and dotted line as previously for one-dimensional deformation. For the sample 3 the function W assumes negative values in a certain range of compression (inadmissible form of W).

Table 1. Material parameters of the stored energy function (7.4) with ψ specified by (7.5) according to [I.50] (rabbit myocardium). The material parameters appearing in (7.7) are also given

No.	C_1	C_2	C_3	C_4	C_1C_2	C_1C_3	C_1C_4
1.	1.01	3.05	−2.24	1.92	3.0805	−2.2624	1.212
2.	2.42	12.13	0.63	1.05	29.3546	1.5246	2.541
3.	9.86	4.62	2.37	0.09	45.5532	23.3682	0.8875
4.	2.92	3.21	−2.60	2.01	9.3732	−7.592	5.8692
5.	2.62	2.40	−0.89	2.01	6.288	−2.3318	5.502
6.	1.67	1.70	1.90	0.38	2.839	3.173	0.6346
7.	6.85	2.88	−0.76	0.38	19.728	−5.206	2.603
8. (averaged values)	1.05	9.13	2.32	0.08	9.5865	2.436	0.084

Similar conclusion applies to the model studied in [I.53], where

$$W = C_0(e^{\tilde{\psi}} - 1), \tag{7.8}$$

and

$$\tilde{\psi} = C_1(I_1 - 3)^2 + C_2(I - 1)^4, \qquad I = \sqrt{I_4} = \sqrt{\mathrm{tr}\mathbf{CM}} = \sqrt{\mathbf{m} \cdot \mathbf{C} \cdot \mathbf{m}}. \tag{7.9}$$

The hyperelastic potential (7.8) was used to model the valve tissue of a pig, which provides a good substitute for similar human tissue. The material parameters,

taken from [I.53], are gathered in Table 2. Now the material functions involved in constitutive relationship (7.6) have the following form:

$$\beta_1 = \frac{\partial W}{\partial I_1} = 2C_0C_1e^{\tilde{\psi}}(I_1 - 3), \qquad \beta_4 = \frac{\partial W}{\partial I_4} = \frac{2C_0C_2}{I}e^{\tilde{\psi}}(I-1)^3. \tag{7.10}$$

We observe that even for relatively large deformations the stored energy function (7.8) with $\tilde{\psi}$ specified by $(7.9)_1$ can be approximated by the following polynomial in I_1 and I:

$$W = C_0C_1(\mathrm{tr}\mathbf{E})^2 + C_0C_2\left(\sqrt{(\mathrm{tr}\mathbf{EM}) - 1} - 1\right)^4. \tag{7.11}$$

Here the independent material parameters C_0C_1 and C_0C_2 can be determined by using linear optimization methods. For the model (7.8) and $(7.9)_1$ the quadratic approximation with respect to the measure $\mathbf{E}$ is useless since it yields an isotropic stored energy function with the first term appearing in (7.11). Figure 18 depicts typical relations between stresses and deformations in one-dimensional test.

Table 2. Material parameters of the stored energy function (7.8), $(7.9)_1$ for the valve tissue of a pig, after [I.53]. The material parameters appearing in (7.11) are also given

No.	C_0 [kPa]	C_1	C_2	C_0C_1 [kPa]	C_0C_2 [kPa]
1	2	3	4	5	6
1.	1.010	2.59	1376.9	2.61590	1514.59
2.	0.079	1.25	1320.6	0.09875	104.3274
3.	0.181	7.01	626.5	1.26881	113.3965
4.	0.214	4.90	1602.9	1.04860	343.0206
5.	0.105	5.23	1991.6	0.54915	209.118
6.	0.203	1.76	833.0	0.35728	169.099
7.	0.053	6.31	1943.2	0.33443	102.9896
8.	2.171	2.19	1408.8	4.75449	3058.5048
9. (averaged values)	0.399	4.325	1446.5	1.725675	577.1535

In the paper [97] the following stored energy function has been implemented in FEM

$$\overline{W}(\overline{I}_1, \overline{I}_2, \overline{I}_3 = C_1(\overline{I}_1 - 3) + C_2(\overline{I}_2 - 3) + C_3\lfloor e^{(\overline{I}_3 - 1)} - \overline{I}_3\rfloor, \tag{7.12}$$

where C_1, C_2 and C_3 are material coefficients whilst the invariants $\overline{I}_i$, $i = 1, 2, 3$, are defined by Eq. (5.10). This model constitutes a simple generalization of the

well-known Mooney-Rivlin potential [I.10, I.58], the last being valid for incompressible isotropic materials. Since the formula (7.12) does not incorporate the invariant $\overline{I}_4$ and there is no coupling between the invariants $\overline{I}_1$ and $\overline{I}_1$, therefore the model (7.12) cannot properly describe incompressible transversely anisotropic materials in the range of small deformations. It seems that the stored energy function (7.12) should be confined to plane problems. WEISS *et al.* [97] devised their model to describe the mechanical behaviour of tendon and cartilage. We observe that from the point of view of FEM, the paper [97] constitutes a first attempt of numerical implementation of the model describing transversely isotropic, hyperelastic and incompressible materials.

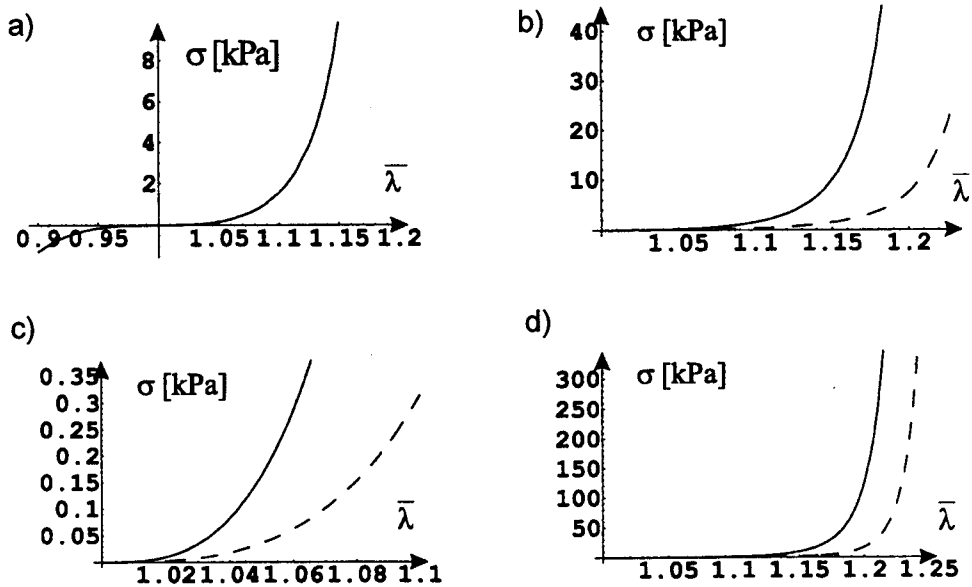

FIG. 18. Cauchy stress-elongation relationships for the one-dimensional extension; the stored energy function is given by (7.8), (7.9). The material parameters are taken from Table 2: continuous line in (a) – (d) after row 9, (b) – sample 3 (dotted line), (c) and (d) – sample 2 (dotted line). The sample orientation coincides with **m**.

8. FINAL REMARKS

Soft tissue modelling ranges from molecular and microscopic levels to application of the methods proper for the continuum mechanics (macroscopic level). New constitutive models proposed in our paper pertain to hyperelastic, isotropic and transversely isotropic soft tissues. The constitutive relations developed in Part II can readily be extended to orthotropic materials.

A striking feature of the models proposed by other authors is the lack of any discussion of mathematical aspects of these models. For instance, such important and well-known notions of mathematical elasticity as polyconvexity, quasiconvexity and rank-one convexity [I.10] of stored energy functions have not yet been assimilated by biomechanical modelling of soft tissues. The notions mentioned are not only mathematically elegant. On the contrary, we are strongly convinced that good models of soft tissues should possess good mathematical properties.

Soft tissues, like bone tissues, are materials with hierarchical architecture. It seems that homogenisation methods, particularly the reiterated homogenisation, could be applied to micro-macro modelling. By passage we observe that the modelling "micro-macro" studied by WREN and CARTER [87] is very crude. These authors studied a geometrically nonlinear behaviour of soft skeletal tissues by considering Voigt and Reuss bounds, well-known in the geometrically linear micromechanics of composites, cf. [10, 63]. The model developed was applied to rabbit tendon bovine menisci and bovine humeral articular cartilage. A poroelastic model developed by VANKAN *et al.* [95] was applied to a simulation of a blood perfused contracting skeletal muscle. Unfortunately, though the model was intended to describe hierarchical media, yet no scaling had been primarily introduced.

There are other interesting topics related to soft tissues, not discussed by us. Let us mention a few, except those alluded to in Part I. First, heat-induced changes seem to be seldom studied, cf. [9] and the references therein. Remodelling of soft tissues and particularly of skeletal muscles is not so frequently studied as bone remodelling, see [I.15, I.16, 42,73, 82, 83]. Soft tissues reveal functional adaptation to loading. For instance, the thickness of arterial wall depends on blood pressure and is larger in the case of the hypertension. The class of soft tissues encompasses various tissues, with various microstructure and fulfilling various functions. Important soft tissues, not discussed in the present two-part paper, are:

(i) cartilage and meniscus, cf. [6, 25, 29, 54],
(ii) annulus fibrosus [22, 23, 45, 51],
(iii) lungs [16, I.15, I.16, I.42, I.45, I.48, I.51, 49, 52],
(iv) ligaments, tendons [I.5, I.30, I.43, I.49, I.78, I.79, 28, 55, 72],
(v) skin [I.4, I.15, I.41, 24, 76].

In Part I we have briefly discussed biological membranes. Here, we additionally mention the papers by HOLZAPFEL *et al.* [35, 36]. Both isotropic and anisotropic membranes were studied.

In the second part of the paper it has been demonstrated that some anisotropic models of hyperelastic soft tissue cannot properly describe the response of such tissues. Similar comment applies to many oversimplified models.

ACKNOWLEDGEMENT

The authors were supported by the State Committee for Scientific Research (KBN, Poland) through the grant No 8 T11F 017 18.

REFERENCES

1. E. S. ALMEIDA, R. L. SPILKER, *Finite element formulation for hyperelastic transversely isotropic biphasic soft tissues*, Comput. Methods Appl. Mech. Engng., **151**, 513–538, 1998.
2. M. BATHE, R. D. KAMM, *A fluid-structure interaction finite element analysis of pulsatile blood flow through a compliant stenotic artery*, J. Biomech. Engng., **121**, 361–369, 1999.
3. D. BEATTIE, C. XU, R. VITO, S. GLAGOV, M. C. WHANG, *Mechanical analysis of heterogeneous, atherosclerotic human aorta*, J. Biomech. Engng., **121**, 602–607, 1998.
4. M. K.-E. BENAOUDA, J. J. TELEGA, *On existence of minimizers for Saint-Venant Kirchhoff bodies: placement boundary condition*, Bull. Pol. Acad. Sci., Tech. Sci., **45**, 211–223, 1997.
5. K. L. BILLIAR, M. S. SACKS, *Biaxial mechanical properties of the natural and glutaraldehyde treated aortic valve cups-Part I: Experimental results*, J. Biomech. Engng., **122**, 23–30, 2000; *Part II: A structural constitutive model*, ibid., 327–335, 2000.
6. P. BURSAČ, C. V. MCGRATH, S. R. EISENBERG, D. STAMENOVIČ, *A microstructural model of elastostatic properties of articular cartilage in confined compression*, J. Biomech. Engng., **122**, 347–353, 2000.
7. M. B. CANNEL, J. R. BERLIN, W. J. LEDERER, *Effect of membrane potential changes on the calcium transient in single rat cardiac muscle cells*, Science, **238**, 1419–1423, 1987.
8. E. D. CAREW, E. A. TALMAN, D. R. BOUGHNER, I. VESELY, *Quasi-linear viscoelastic theory applied to internal shearing of porcine aortic valve leaflets*, J. Biomech. Engng., **121**, 386–392, 1999.
9. S. S. CHEN, J. D. HUMPHREY, *Heat-induced changes in the mechanics of a collagenous tissue: pseudoelastic behavior at C*, J. Biomech., **31**, 211–216, 1998.
10. A. CHERKAEV, *Variational methods for structural optimization*, Springer-Verlag, New York 2000.
11. C. J. CHUONG, Y. C. FUNG, *Three-dimensional stress distribution in arteries*, J. Biomech. Engng., **105**, 268–274, 1983.
12. C. J. CHUONG, Y. C. FUNG, *Residual stress in arteries*, [In:] *Frontier in biomechanics*, G. W. SCHMID-SCHÖNBEIN, S. L.-Y. WOO and B. W. ZWEIFACH [Eds.], pp. 117–129, Springer-Verlag, New York 1986.
13. C. J. CHUONG, Y. C. FUNG, *Residual stress in arteries*, J. Biomech. Engng., **108**, 189–192, 1986.
14. K. D. COSTA, F. C. P. YIN, *Analysis of indentation: implications for measuring mechanical properties with atomic force microscopy*, J. Biomech. Engng., **121**, 462–471, 1999.
15. H. DEMIRAY, R. P. VITO, *A layered cylindrical shell model for an aorta*, Int. J. Engng. Sci., **29**, 47–54, 1991.

16. E. DENNY, R. C. SCHROTER, *Viscoelastic behavior of a lung alveolar duct model*, J. Biomech. Engng., **122**, 143–151, 2000.

17. K. A. DERWIN, L. J. SOSLOWSKY, *A quantitative investigation of structure-function relationships in a tendon fascile model*, J. Biomech. Engng., **121**, 598–604, 1999.

18. G. V. DIMITROV, N. A. DIMITROVA, *Fundamentals of power spectra of extracellular potentials produced by a skeletal muscle fibre of finite length. Part I: Effect of fibre anatomy*, Med. Engng. Physics, **20**, 580–587, 1998, *Part II: Effect of parameters altering with functional state*, ibid., 702–707.

19. G. V. DIMITROV, N. A. DIMITROVA, *Effect of parameters altering with muscle fibre functional state on the power spectra of spatially filtered extracellular potentials*, J. Med. Engng. Technol., 2001, in press.

20. N. A. DIMITROVA, G. V. DIMITROV, O. A. NIKITIN, *Longitudinal variations of characteristic frequencies of skeletal muscle fibre potentials detected by a bipolar electrode or multielectrode*, J. Med. Engng. Tech., 2001, in press.

21. S. DOKOS, I. J. LEGRICE, B. H. SMAILL, J. KAR, A. A. YOUNG, *A triaxial-measurement shear device for soft biological tissues*, J. Biomech. Engng., **122**, 471–478, 2000.

22. R. EBERLEIN, G. A. HOLZAPFEL, C. A. J. SCHULZE-BAUER, *An anisotropic constitutive model for annulus tissue and enhanced finite element analyses of intact lumbar disc bodies*, Comp. Meth. Biomech. Biomed. Engng., in press.

23. D. M. ELLIOT, L. A. SETTON, *A linear model for fiber-induced anisotropy of the anulus fibrosus*, J. Biomech. Engng., **122**, 173–179, 2000.

24. D. M. FLYNN, G. D. PEURA, P. GRIGG, A. H. HOFFMAN, *A finite element based method to determine the properties of planar soft tissue*, J. Biomech. Engng., **120**, 202–210, 1998.

25. M. FORTIN, J. SOULHAT, A. SHIRAZI-ADL, E. B. HUNZIKER, M. D. BUSCHMANN, *Unconfined compression of articular cartilage: nonlinear behavior and comparison with a fibre-reinforced biphasic model*, J. Biomech. Engng., **122**, 189–195, 2000.

26. Y. C. FUNG, S. Q. LIU, *Change of residual strains in arteries due to hypertrophy caused by aortic constriction*, Circulation Res., **65**, 1340–1349, 1989.

27. Y. C. FUNG, S. Q. LIU, *Changes of zero-stress state of rat pulmonary arteries in hypoxic hypertension*, J. Appl. Physiol., **70**, 2455–2470, 1991.

28. J. R. FUNK, G. W. HALL, J. R. CRANDALL, W. D. PILKEY, *Linear and quasi-linear viscoelastic characterization of ankle ligaments*, J. Biomech. Engng., **122**, 15–22, 2000.

29. A. GAŁKA, J. J. TELEGA, R. WOJNAR, *Electromechanical modelling of cartilage*, Engng. Trans., this issue.

30. S. E. GREENWALD, J. E. MOORE, A. RACHEV, T. P. C. KANE, J.-J. MEISTER, *Experimental investigation of the distribution of residual strains in the artery wall*, J. Biomech. Engng., **119**, 438–444, 1997.

31. H. GREGERSEN, T. C. LEE, S. CHIEN, R. SKALAK, Y.C. FUNG, *Strain distribution in the layered wall of the esophagus*, J. Biomech. Engng., **121**, 442–448, 1999.

32. J. M. GUCCIONE, A. D. MCCULLOCH, *Finite element modeling of ventricular mechanics* [In:] *Theory of heart*, L. GLASS, P. HUNTER and A. MCCULLOCH [Eds.], 121–144, Springer-Verlag, New York 1991.

33. M. HAJJAR, W. MÊME, C. LÉOTY, *Measurement of sarcomere length during fast contraction of muscle fibers by digital image analysis*, J. Biomechanics, **32**, 737–742, 1999.

34. H. C. HAN, Y. C. FUNG, *Direct measurement of transverse residual strain in aorta*, Amer. J. Physiol., **270**, (Heart Circ. Physiol., **39**), H750–H759, 1996.

35. G. A. HOLZAPFEL, R. EBERLEIN, P. WRIGGERS, H. W. WEIZSÄCKER, *Large strain analysis of soft biological membranes: formulation and finite element analysis*, Compt. Methods Appl. Mech. Engng., **132**, 45–61, 1996.

36. G. A. HOLZAPFEL, R. EBERLEIN, P. WRIGGERS, H. W. WEIZSÄCKER, *A new axisymmetrical membrane element for anisotropic finite strain analysis of arteries*, Comm. Numer. Meth. Engng., **12**, 507–517, 1996.

37. G. A. HOLZAPFEL, T. C. GASSER, *A viscoelastic model for fiber-reinforced composites at finite strain: Continuum basis, computational aspects and applications*, Comput. Methods Appl. Mech. Engng., in press.

38. G. A. HOLZAPFEL, T. C. GASSER, R. W. OGDEN, *A new constitutive framework for arterial wall mechanics and a comparative study of material models*, J. Elasticity, in press.

39. G. A. HOLZAPFEL, C. A. J. SCHULZE-BAUER, M. STADLER, *Mechanics of angioplasty: wall balloon and stent* [In:] *Mechanics in biology*, J. CASEY and G. BAO [Eds.], 141–156, AMD-vol. 242, The American Society of Mechanical Engineers, New York 2000.

40. G. A. HOLZAPFEL, H. W. WEIZSÄCKER, *Biomechanical behavior of the arterial wall and its numerical characterization*, Computers in Biol. Med., **28**, 377–392, 1998.

41. A. HOROWITZ, *Structural considerations in formulating material laws for the myocardium* [In:] *Theory of heart*, L. GLASS, P. HUNTER and A. MCCULLOCH [Eds.], 31–58, Springer-Verlag, New York 1991.

42. J. D. HUMPHREY, *Remodeling of a collagenous tissue at fixed lengths*, J. Biomech. Engng., **121**, 591–597, 1999.

43. J. D. HUMPHREY, *An evaluation of pseudoelastic descriptors used in arterial mechanics*, J. Biomech. Engng., **121**, 259–262, 1999.

44. J. M. HUYGHE, T. ARTS, D. H. VAN CAMPEN, R. S. RENEMAN, *Porous medium finite element model of the beating left ventricle*, Amer. J. Physiol., **262**, (Heart Circ. Physiol., **31**), H1256–H1267, 1992.

45. J. C. IATRIDIS, L. A. SETTON, R. J. FOSTER, B. A. RAWLINS, M. WEIDENBAUM, V. C. MOW, *Degeneration affects the anisotropic and nonlinear behaviours of human anulus fibrosus in compression*, J. Biomechanics, **31**, 535–544, 1998.

46. S. JEMIOŁO, J. J. TELEGA, C. MICHALAK, *Hyperelastic anisotropic models of soft tissues*, Acta Bioeng. Biomech., **2**, Supplement 1, 235–240, 2000.

47. S. JEMIOŁO, J. J. TELEGA, *On finite anisotropic hyperelasticity and applications to soft tissue modelling* [In:] Polish-Ukrainian Transactions " Theoretical Foundations in Civil Engineering, W. SZCZEŚNIAK [Ed.], 319–330, Oficyna Wydawnicza Politechniki Warszawskiej, Warszawa 2000.

48. S. JEMIOŁO, J. J. TELEGA, *Modelling elastic behaviour of soft tissues. Part I. Isotropy*, Engng. Trans., **49**, 2–3, 213–240, 2001.

49. A. D. KARAKAPLAN, M. P. BIENIEK, R. SKALAK, *A mathematical model of lung parenchyma*, J. Biomech. Engng., **102**, 124–136, 1980.

50. V. A. KAS'YANOV, A. I. RACHEV, *Deformation of blood vessels upon stretching, intramural pressure and torsion*, Mech. Comp. Mater., **16**, 76–80, 1980.

51. S. M. KLISCH, J. C. LOTZ, *A special theory of biphasic mixtures and experimental results for human annulus fibrosus tested in confined compression*, J. Biomech. Engng., **122**, 181–188, 2000.

52. E. KIMMEL, R. D. KAMM, A. H. SHAPIRO, *A cellular model of lung elasticity*, J. Biomech. Engng., **109**, 126–131, 1987.

53. A. KIRPALANI, H. PARK, J. BUTANY, K. W. JOHUSTON, M. OJHA, *Velocity and wall shear stress patterns in the human right coronary artery*, J. Biomech. Engng., **121**, 370–375, 1999.

54. W. M. LAI, V. C. MOW, D. D. SUN, G. A. ATESHIAN, *On the electric potentials inside a charged hydrated biological tissue: streaming potential versus diffusion potential*, J. Biomech. Engng., **122**, 336–346, 2000.

55. R. S. LAKES, R. VANDERBY, *Interrelation of creep and relaxation: a modeling approach for ligaments*, J. Biomech. Engng., **121**, 612–615, 1999.

56. C. S. LEE, J. M. TARBELL, *Wall shear rate distribution in an abdominal aortic bifurcation model: effects of vessel compliance and phase angle between pressure and flow waveforms*, J. Biomech. Engng., **119**, 333–342, 1997.

57. J. D. LEMMON, A. P. YOGANATHAN, *Three-dimensional computational model of left heart diastolic function with fluid-structure interaction*, J. Biomech. Engng., **122**, 109–117, 2000.

58. J. D. LEMMON, A. P. YOGANATHAN, *Computational modelling of left heart diastolic function: examination of ventricular dysfunction*, J. Biomech. Engng., **122**, 297–303, 2000.

59. W. Y. W. LEW, *Functional consequences of regional heterogeneity in the left ventricle* [In:] *Theory of heart*, L. GLASS, P. HUNTER and A. MCCULLOCH [Eds.], 209–237, Springer-Verlag, New York 1991.

60. S. Q. LIU, Y. C. FUNG, *Zero-stress state of arteries*, J. Biomech. Engng., **110**, 82–84, 1988.

61. S. Q. LIU, Y. C. FUNG, *Relationship between hypertension, hypertrophy, and opening angle of zero-stress state of arteries following aortic constriction*, J. Biomech. Engng., **111**, 325–335, 1989.

62. A. D. MCCULLOCH, J. H. OMENS, *Factors affecting the regional mechanics of the diastolic heart* [In:] *Theory of heart*, L. GLASS, P. HUNTER and A. MCCULLOCH [Eds.], 87–119, Springer-Verlag, New York 1991.

63. G. W. MILTON, *The theory of composites*, Laminated Publishers, New York, in press.

64. B. S. MYERS, C. T. WOOLLEY, T. L. SLOTTER, W. E. GARRETT, T. M. BEST, *The influence of strain rate on the passive and stimulated engineering stress-large strain behavior of the rabbit tibialis anterior muscle*, J. Biomech. Engng., **120**, 126–132, 1998.

65. P. NIELSEN, I. HUNTER, *Identification of the time-varying properties of the heart* [In:] *Theory of heart*, L. GLASS, P. HUNTER and A. MCCULLOCH [Eds.], 77–86, Springer-Verlag, New York 1991.

66. R. W. OGDEN, C. A. J. SCHULZE-BAUER, *Phenomenological and structural aspects of the mechanical response of arteries* [In:] *Mechanics in biology*, J. CASEY and G. BAO [Eds.], 125–140, AMD-vol. 242, The American Society of Mechanical Engineers, New York 2000.

67. R. W. OGDEN, P. G. ROXBURGH, *A pseudo-elastic model for the Mullins effect in filled rubber*, Proc. R. Soc., **A455**, 2861–2877, London 1999.

68. R. J. OKAMOTO, M. J. MOULTON, S. J. PETERSON, D. LI, M. K. PASQUE, J. M. GUCCIONE, *Epicardial suction: a new approach to mechanical testing of the passive ventricular wall*, J. Biomech. Engng., **122**, 479–487, 2000.

69. J. H. OMENS, Y.-C. FUNG, *Residual strain in rat left ventricle*, Circulation Res., **66**, 37–45, 1990.

70. E. M. ORTT, D. J. DOSS, E. LEGALL, N. T. WRIGHT, J. D. HUMPHREY, *A device for evaluating the multiaxial finite strain thermomechanical behavior of elastomers and soft tissues*, J. Appl. Mech., **67**, 465–471, 2000.

71. S. J. PETERSON, R. J. OKAMOTO, *Effect of residual stress and heterogeneity on circumferential stress in the arterial wall*, J. Biomech. Engng., **122**, 454–456, 2000.

72. K. M. QUAPP, J. A. WEISS, *Material characterization of human medial collateral ligament*, J. Biomech. Engng., **120**, 757–763, 1998.

73. A. RACHEV, N. STERGIOPULOS, J.-J. MEISTER, *A model for geometric and mechanical adaptation of arteries to sustained hypertension*, J. Biomech. Engng., **120**, 9–17, 1998.

74. T. F. ROBINSON, L. COHEN-GOULD, S. M. FACTOR, *Skeletal framework of mammalian heart muscle: arrangement of inter-and peri-cellular connective tissue structures*, Lab. Invest., **49**, 482–498, 1983.

75. T. F. ROBINSON, S. M. FACTOR, E. H. SONNENBLICK, *The heart as a suction pump*, Scientific Amer., **254**, 84–91, 1986.

76. M. B. RUBIN, S. R. BODNER, N. S. BINUR, *An elastic-viscoplastic model for excised facial tissues*, J. Biomech. Engng., **120**, 686–689, 1998.

77. M. S. SACKS, *A method for planar biaxial mechanical testing that includes in-plane shear*, J. Biomech. Engng., **121**, 551–555, 1999.

78. M. S. SACKS, *Tissue-level structural constitutive models* [In:] *Mechanics in biology*, J. CASEY and G. BAO [Eds.], 113–124, AMD-vol. 242, The American Society of Mechanical Engineers, New York 2000.

79. L. A. SETTON, H. TOHYAMA, V. C. MOW, *Swelling and curling behaviors of articular cartilage*, J. Biomech. Engng., **120**, 355–361, 1998.

80. B. H. SMAILL, P. J. HUNTER, *Structure and function of the diastolic heart* [In:] *Theory of heart*, L. GLASS, P. HUNTER and A. MCCULLOCH [Eds.], 1–29, Springer-Verlag, New York 1991.

81. S. R. SUMMEROUR, J. L. EMERY, B. FAZELI, J. H. OMENS, A. D. MCCULLOCH, *Residual strain in ischemic ventricular myocardium*, J. Biomech. Engng., **120**, 710–714, 1998.

82. L. A. TABER, *Biomechanics of growth remodeling, and morphogenesis*, Appl. Mech. Reviews, **48**, 487–545, 1995.

83. L. A. TABER, *A model for aortic growth based on fluid shear and fiber stresses*, J. Biomech. Engng., **120**, 348–354, 1998.

84. E. TANAKA, H. YAMADA, S. MURAKAMI, *Inelastic constitutive modeling of arterial and ventricular walls* [In:] *Computational biomechanics*, K. HAYASHI and H. ISHIKAWA [Eds.], 137–163, Springer-Verlag, Tokyo 1996.

85. D. TANG, J. YANG, C. YANG, D. N. KU, *A nonlinear axisymmetric model with fluid-wall interactions for steady viscous flow in stenotic tubes*, J. Biomech. Engng., **121**, 494–501, 1999.

86. L. K. WALDMAN, *Multidimensional measurement of regional strains in the intact heart* [In:] *Theory of heart*, L. GLASS, P. HUNTER and A. MCCULLOCH [Eds.], 145–174, Springer-Verlag, New York 1991.

87. T. A. L. WREN, D. R. CARTER, *A microstructural model for the tensile constitutive and failure behavior of soft skeletal connective tissues*, J. Biomech. Engng., **120**, 55–61, 1998.

88. K. TAKAMIZAWA, K. HAYASHI, *Constitutive law of the arterial wall and stress distribution* [In:] *Computational mechanics 86: theory and applications*, G. YAGAWA and S. N. ATLURI [Eds.], (IV-149)–(IV-154), Springer-Verlag, Tokyo 1986.

89. K. TAKAMIZAWA, K. HAYASHI, *Strain energy density function and uniform strain hypothesis for arterial mechanics*, J. Biomechanics, **20**, 7–17, 1987.

90. K. TAKAMIZAWA, K. HAYASHI, *Uniform strain hypothesis and thin-walled theory in arterial mechanics*, Biorheology, **25**, 555–565, 1988.

91. K. TAKAMIZAWA, T. MATSUDA, *Kinematics for bodies undergoing residual stress and its applications to the left ventricle*, J. Appl. Mech., **57**, 321–329, 1990.

92. R. N. VAISHNAV, J. VOSSOUGHI, *Estimation of residual strains in aortic segments* [In:] *Biomedical Engineering II, Recent Developments*, C. W. HALL [Ed.], 330–333, Pergamon Press, New York 1983.

93. J. VALENTA, T. HRU, M. SOCHOR, *Residual stresses in the human aorta and their influence by growth and remodelling*, Bio-Med. Mat. Engng., **7**, 159–169, 1997.

94. C. A. VAN EE, A. L. CHASSE, B. S. MYERS, *Quantifying skeletal muscle properties in cadaveric test specimens: effects of mechanical loading, postmortem time and freezer storage*, J. Biomech. Engng., **122**, 9–14, 2000.

95. V. J. VANKAN, J. M. HUYGHE, J. D. JANSSEN, A. HUSON, *Poroelasticity of saturated solids with an application to blood perfusion*, Int. J. Engng. Sci., **34**, 1019–1031, 1996.

96. J. VOSSOUGHI, Z. HEDJAZI, F. S. BORRIS, *Intimal residual stress and strain in large arteries* [In:] BED-vol. 24, Proc. ASME Summer Bioengineering Conference, Breckenridge, 434–437, 1993.

97. J. A. WEISS, B. N. MAKER, S. GOVINDJEE, *Finite element implementation of incompressible, transversely isotropic hyperelasticity*, Comp. Meth. Engng. Appl. Mech. Engng., **135**, 107–128, 1996.

98. A. YOUNG, *Epicardial deformation from coronary cinéagiograms, in: Theory of heart*, L. GLASS, P. HUNTER and A. MCCULLOCH [Eds.], 175–207, Springer-Verlag, New York 1991.

99. G. I. ZAHALAK, V. DE LABORDERIE, *The effects of cross-fiber deformation on axial fiber stress in myocardium*, J. Biomech. Engng., **121**, 376–385, 1999.

100. S. Z. ZHAO, X. Y. XU, M. W. COLLINS, *The numerical analysis of fluid-solid interactions for blood flow in arterial structures. Part 1: A review of models for arterial wall behaviour*, Proc. Instn. Mech. Engrs, **212**, Part H, 229–240, 1998; *Part 2: Development of coupled fluid-solid algorithms*, ibid., 241–252.

101. J. MACKERLE, *A finite element bibliography for biomechanics (1987-1997)*, Appl. Mech. Reviews, **51**, 587–634, 1998.

102. J. H. OMENS, S. M. VAPLON, B. FAZELI, A. D. MCCULLOCH, *Left ventricular geometric remodeling and residual stress in the rat heart*, J. Biomech. Engng., **120**, 715–719, 1998.

Received March 30, 2001.